The nearshore wind and wave energy potential of Ireland: a high resolution assessment of availability and accessibility

Sarah Gallagher[a,b], Roxana Tiron[b,1], Eoin Whelan[a], Emily Gleeson[a], Frédéric Dias[b,c,*], Ray McGrath[a]

[a] *Met Éireann, Glasnevin, Dublin 9, Ireland*
[b] *UCD School of Mathematics and Statistics, University College Dublin, Belfield, Dublin 4, Ireland*
[c] *Centre de Mathématiques et de Leurs Applications, École Normale Supérieure de Cachan, 94235, France*

Abstract

A 14-year high resolution wave and wind hindcast was carried out for Ireland. The wind was dynamically downscaled from the ERA-Interim reanalysis to a 2.5 km horizontal resolution and 65 vertical levels, using the HARMONIE meso-scale model. The wave hindcast was derived using WAVEWATCH III on an unstructured grid with resolution ranging between 10 km offshore and 225 m in the nearshore, forced by the downscaled HARMONIE 10 m winds and ERA-Interim wave spectra. The wind and wave hindcasts were thoroughly validated against available buoy data, including wave buoys in nearshore locations and coastal synoptic stations. In addition, the significant wave heights and winds from the hindcasts were compared against all available altimeter data from the CERSAT database at Ifremer. The quality of both the wind and wave hindcasts was found to be good.

The wave and wind energy resource in coastal areas was assessed, and discussed in terms of water depth, distance to shore, and seasonal and inter-annual variability. In addition, the current study investigates the nearshore wind and wave climate in conjunction with each other, and highlights two issues with relevance to the ocean renewable energy industry: (i) the complementarity between the wind and wave energy resource, and (ii) the accessibility for marine operations. Our study highlights sites around the Irish coast that might have been overlooked in terms of the potential for wind, wave or

*Tel: +353 1 716 2559
Email address: frederic.dias@ucd.ie (Frédéric Dias)
[1]Current affiliation: OpenHydro Ltd., Greenore, Co. Louth, Ireland

combined wind/wave energy installations.

Keywords: wave energy resource, wind energy resource, high-resolution regional model, complementarity, weather windows, Ireland

1. Introduction

From an offshore renewable energy perspective, a country like Ireland in the Atlantic Ocean, is uniquely placed in Europe in terms of its wind and wave energy resource. As part of the Irish government's overall target of achieving 40 per cent of electricity generated from renewables by 2020, a 500 MW target for installed ocean wave capacity by 2020 [1] has been set. The *Offshore Renewable Energy Development Plan* for Ireland [2] which was launched in February 2014, aims to encourage developments for Ocean Energy (OE) at a national level.

The ESB's WestWave [3] project has also secured funding under the EU's New Entrant Reserve (NER300) scheme and plans are underway to install a 5 MW demonstrative Wave Energy Converter (WEC) farm off the west coast. In addition, the development of ocean energy test sites off the west coast of Ireland (a quarter-scale test site in Galway Bay, a full-scale test site in Belmullet – the Atlantic Marine Energy Test Site AMETS) and the new Marine Renewable Energy Ireland SFI Research Centre (MaREI) [4], ensures that Ireland continues to develop its position as a potential global leader in marine renewable energy into the future.

At a European level, 4.9 GW of offshore wind power capacity is under construction [5]. In Ireland, there are currently seven turbines (with 25 MW power capacity) installed in a wind farm on the Arklow Bank, off the east coast of Ireland in the Irish Sea. Additional foreshore leases have been granted for the Arklow Bank and another site on the Codling Bank (also off the east coast, see Figure 1) with a combined power capacity of 1620 MW. Another tranche of offshore wind projects are currently seeking foreshore leases for projects around the coast, such as the Oriel Windfarm and the Dublin Array (Kish Bank) on the east coast and Fuinneamh Sceirde Teoranta on the west coast, near Mace Head [6, 7].

In this context, it is paramount to have an accurate picture of the available wave and wind energy resource, and thus, of the potential energy yields from these developments. Furthermore, this knowledge is necessary for the selection of additional OE sites in Ireland. Data from a small number of buoy or coastal weather stations provide detailed information at specific sites, but over large areas there is a general lack of detailed information. In addition to the few wave buoys and weather stations, most of our wave climate knowledge is currently based on deep water, coarse resolution models or limited area models (targeting potential wave energy testing and deployment sites) which are not appropriate sources in this context. Apart from the high-resolution, long-term wave hindcast, driven by ERA-Interim wave spectra and winds, carried out by [8] for Ireland (both the Atlantic and the Irish Sea coast), there are several other studies limited to small nearshore sites, [9, 10, 11] or offshore locations on the Irish west coast, [12, 13, 14]. The wind energy potential of Ireland has been previously assessed (for example, the SEAI wind atlas for Ireland [15]). Furthermore, a 40-year downscaling of ERA-40 atmospheric dataset [16] for Ireland has been performed in [17] resulting in a 13 km horizontal grid spacing with 40 vertical levels.

It should be noted that the wind and wave studies for Ireland mentioned above do not always cover concurrent periods and have disparate resolutions. Additionally, some nearshore/coastal areas of interest around Ireland have not yet been modelled to a high-resolution. At the same time, targeting areas in the nearshore/coastal regions can enhance OE viability for at least two reasons: (i) device survivability and (ii) reduced cost in transporting this energy to the shore. In fact, accessibility for deployment and maintenance is proving to be a key factor in the successful development of OE devices. Apart from an accurate assessment of the energy resource, building a joint picture of met-ocean conditions (both wind and wave) is crucial. The complementarity between both wind and wave power also has the potential to reduce transmission requirements [18, 19].

The paper is organised as follows. Details of the wind and wave model data and method of implementation are presented in Section 2. (The wind and wave model validation is included in Appendix A.) In Section 3 we discuss the wind and wave energy resource around the Irish coast and the complementarity between the two, whereas in Section 4, we assess the accessibility for marine operations. In Section 5 we discuss the results of the study and finally, in Section 6, we summarise and conclude our findings.

2. Data and Methodology

To accurately represent coastal features (quite complex in the case of Ireland) climate hindcasts of high spatial resolution, properly calibrated against available measurements are indispensable. To address these requirements, we have performed a high-resolution, 14-year (2000–2013) wave and wind climate hindcasts for Ireland (both the Atlantic, Celtic Sea and Irish Sea coasts), with a focus on the nearshore areas. We have adopted a dynamical downscaling approach using the ERA-Interim re-analysis data-set [20], from the European Centre for Medium Range Weather Forecasts (ECMWF) as forcing for high-resolution regional-area atmospheric and wave models (HARMONIE and WAVEWATCH III, respectively).

The wind hindcast was derived by using a high-resolution limited-area atmospheric model (LAM) to downscale the ERA-Interim Atmospheric re-analysis. This was carried out using the meso-scale HARMONIE model [21, 22], a well-established atmospheric model used by Met Éireann for operational forecasting.

The wave climate was estimated using the third generation spectral wave model WAVEWATCH III® version 4.11 [23], the unstructured grid formulation [24]. In order to provide a realistic description of the nearshore waves, the wave model was driven by the HARMONIE downscaled 10 m winds, which have sufficient resolution to reflect the small scale orographic features associated with the coastlines and the sheltering effects of bays and islands. The wave hindcast was forced at the boundaries by high-quality boundary input consisting of wave directional spectra from the ERA-Interim global wave re-analysis.

An analysis of the wave and wind energy resource in coastal areas was performed, focusing on the availability and accessibility in terms of water depth and the distance to shore. The wave energy resource estimates were computed directly from the wave variance spectrum avoiding parametric formulas (based on assumed spectral shape) and incorporating finite depth effects. Given the high vertical resolution of the HARMONIE model (65 levels), the wind power was calculated directly from the model outputs, with no assumptions regarding the vertical profile of the wind.

2.1. Implementation of the HARMONIE mesoscale model for Ireland

The HARMONIE model is a non-hydrostatic, convection-permitting model developed by the HIRLAM consortium in cooperation with Météo-France and the ALADIN consortium [22, 25]. HARMONIE largely builds upon model components that were initially developed in these two communities. At the default horizontal grid spacing of 2.5 km, the forecast model and analysis system are basically those of the AROME model from Météo-France. The downscaling area covers all of Ireland and its coastal waters ensuring that physically consistent wind fields are generated for both land and sea areas. The downscaling process assimilates surface weather observations for further consistency.

For the hindcast HARMONIE cycle 37h1.2 was configured to run on an horizontal grid of 2.5 km, using 65 vertical levels, with a model top of 10 hPa. The model domain was centred over the Island of Ireland on a rotated Lambert Conic Conformal projection. Separate simulations were set up to run for one year at a time, with a one-month spin-up period for each simulation. ERA-Interim re-analysis data [20] were used for the lateral boundary conditions (LBCs).

ERA-Interim is a re-analysis of the global atmosphere covering the period from 1 January 1979 to the present [20, 26]. The ERA-Interim atmospheric model uses cycle 31r2 of the ECMWFs Integrated Forecast System (IFS) and has 60 vertical levels with a model top at 0.1 hPa, a T255 spherical-harmonic representation of the dynamical fields and a reduced Gaussian grid with horizontal a resolution of approximately 79 km for surface fields. Note that synoptic land station surface pressure and relative humidities were assimilated into ERA-INTERIM. Surface pressure and 10m winds from drifting buoys and ships were also assimilated [20].

The observations (land) used in the surface data assimilation scheme are the same as those used by ERA-Interim. A 6-hour forecast cycle with surface data assimilation was used. No upper-air data assimilation was carried out, but large scale information from the lateral boundary conditions were blended into the model at the start of each forecast cycle. The information from the ERA-Interim LBCs were read in by HAR-

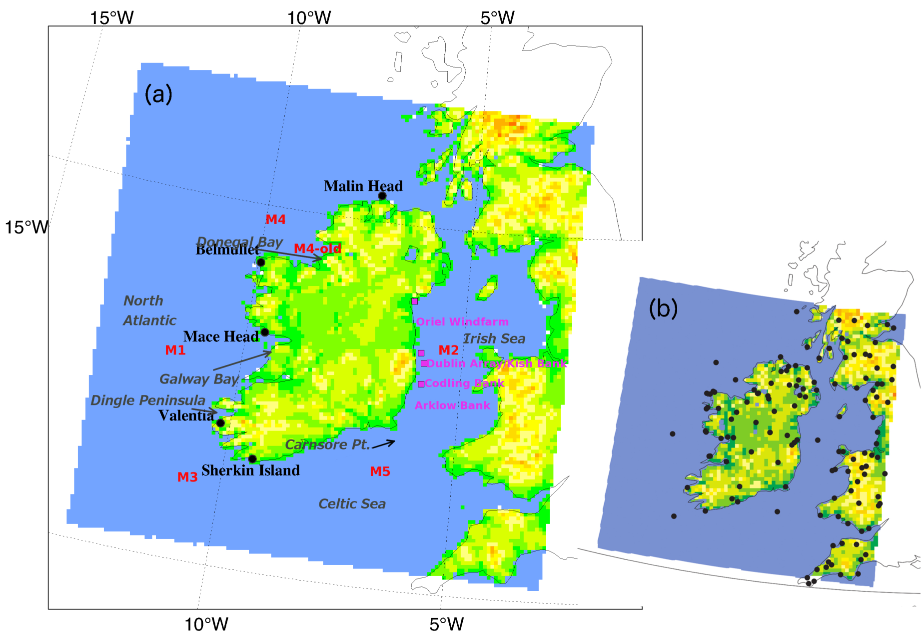

Figure 1: (a) The horizontal grid of the HARMONIE model with the location of the coastal land synoptic stations (Malin Head, Belmullet, Mace Head, Valentia and Sherkin Island denoted with black circle markers) maintained by Met Éireann, and used for validation of the 10 m HARMONIE downscaled winds. Wind data from the M-buoys (denoted in red) from the Irish Marine Weather Buoy Network were also used for validation (also see Figure 2 for their locations). Windfarm locations in the Irish Sea are denoted with magenta square markers. Geographical locations of interest are labelled in grey. (b) The locations of the full network of surface stations used in the HARMONIE model 10 m wind validation (>120 stations).

MONIE forecast once an hour using one-way nesting. The downscaling ratio, the ratio of the driving model (ERA-Interim) grid spacing to the LAM (HARMONIE) grid spacing, is approximately 32:1. Ideally, the resolution of LBC data and the LAM should be as close as possible [27]. Idealised studies have described the problem of reflections at outflow boundaries when there is a mismatch in resolutions [28]. [29] showed that using downscaling ratios of up to 4:1 LBC errors are small and confined to the boundaries. However, downscaling of global climate simulations have used a downscaling factor of 17 [30] and a recent project to produce an extreme wind climatology for The Netherlands using ERA-Interim and HARMONIE [31] have shown that the approach taken by this study, nesting HARMONIE directly with ERA-Interim LBCs, to be effective.

2.2. Implementation of WAVEWATCH III for Ireland

The WAVEWATCH III wave model grid was generated using the open source software PolyMesh [32]. The wave model parameterisation schemes chosen for the input and dissipation terms were formulated as per [33], using the *TEST451* formulation which has been tuned for ECMWF global winds [23]. The wave model grid is an unstructured triangular grid with grid spacing varying from 225 m in the nearshore to 10 km in the offshore. We have used the same Digital Elevation Model (DEM) as in [8]. The DEM blends three bathymetric sources : (i) vector data derived from the United Kingdom Hydrological Office (UKHO) admiralty charts, (ii) the European Marine Observation and Data Network bathymetric dataset EMODnet [34] and (iii) high resolution MBES and LIDAR INFOMAR survey data [35] (approximately 50 gridded datasets, with resolutions from 2 m to 80 m).

The coast and island boundaries were derived from the Ordnance Survey of Ireland (OSI) high-water mark (HWM) vector dataset [36]. The coastline was smoothed and sampled at approximately 200 m. Geo-referenced satellite imagery [37] along with bathymetry from the DEM (de-tided to Mean Sea Level MSL) was used to check the coastline and islands. In many areas, high resolution bathymetry is not available beyond the 5 m or 10 m depth contour; therefore a limiting bottom depth for the wave model was set at 5 m.

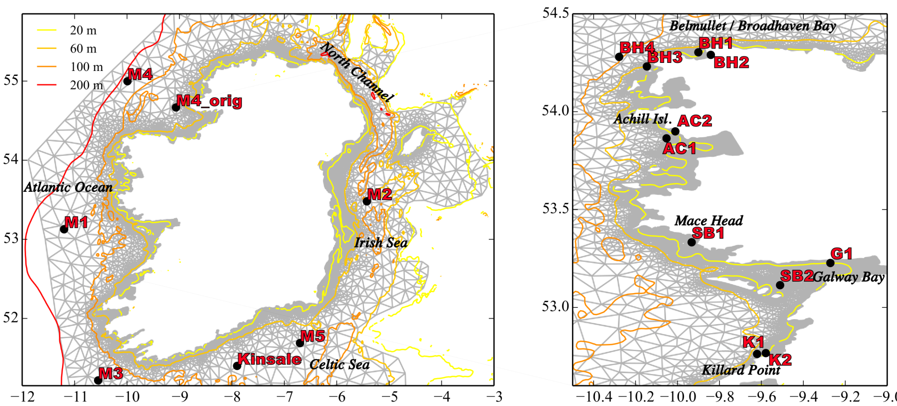

Figure 2: The wave model grid with 20,235 nodes, and the locations of the buoys used for validation. The 20, 60, 100 and 200 m isobaths are marked to indicate the general depths where the buoys are located around the coast. Details about the precise location (latitude/longitude) and the duration of the datasets used for the wave model validation are given in Table A.2.

The resulting grid has approximately 20,000 nodes with a maximum resolution of 225 m in the nearshore (see Figure 2). The outer boundary of the grid was chosen to align with the ERA-Interim wave model grid points.

The boundary forcing consists of ERA-Interim re-analysis wave spectra. The ERA-Interim atmospheric model is two-way coupled to the ocean wave model with a spectral resolution of 30 frequencies and 24 directions and a spatial resolution of $1° \times 1°$ on a reduced latitude/longitude grid [20]. The boundary feeding was set at the wave model grid nodes on the open boundary (in between, and at, the ERA-Interim grid points), where depths were larger than 90 m. The spectral domain was discretized in 24 directions and 30 frequencies logarithmically spaced with an increment of 1.1 from 0.0345 Hz, which coincides with the resolution of the ERA-Interim wave spectra used to force the model. The temporal resolution of the boundary feeding is 6 hours, at the four standard synoptic times of 00:00, 06:00, 12:00 and 18:00 UTC [20].

2.3. Validation of HARMONIE and WAVEWATCH III

The wind and wave hindcasts were thoroughly validated against available buoy data, including wave buoys in nearshore locations off the west coast and coastal and inland synoptic stations. In addition, the hindcasts were compared to all available altimeter data for significant wave height and surface winds from the CERSAT database at Ifremer [38, 39]. The quality of both wind and wave hindcast data were found to be good.

Using the downscaled HARMONIE winds as forcing, the quality of the wave model results improved with respect to [8] (forced with ERA-Interim winds) in sheltered areas around the coast (such as Galway Bay) and in the Irish Sea. Significant improvements were found at the M2, M4 old location and M5 buoys. The HARMONIE 10 m winds were found to be generally superior (to ERA-Interim) in predicting both wind intensity and directionality, in particular at the coastal land stations. A reduction in the bias of 1 m/s and the RMSE of 0.5 m/s for the 10 m wind speed; and 4° in the directional bias was found over all surface stations combined compared to ERA-Interim (see Figure A.13). For full description of the validation procedure and results see Appendix A.

3. Assessment of the wave and wind energy resource

In the following we assess the wind (in Section 3.1) and wave (in Section 3.2) energy resources for Ireland, based on the 14-year hindcast covering the period 2000–2013. We examine regions of interest for wind and wave energy around the coast with a focus on the nearshore, analysing the variability of the resource across bathymetric depth contours (isobaths). We also examine the variability by season (winter, DJF - December, January, February; spring, MAM - March, April, May; summer, JJA - June, July, August; autumn, SON - September, October, November). We have defined 5 nearshore regions (marked in Figure 3): the northwest (NW), west (W), southwest (SW), south (S) and east (E). Finally, in Section 3.3 we consider the joint wind and wave energy resource, in an effort to isolate regions where the resource is complementary and hence propitious for joint wind-wave farm installations.

3.1. Wind resource

When estimating energy return levels for offshore installations, in particular while considering grid integration strategies and how the wind power resource will fit in the overall national energy balance, it is important to quantify not only the average energy resource but also the expected variability. This can occur at various temporal scales: seasonal, annual and even inter-decadal. The temporal extent of the hindcast is too short to assess the latter (this has been done for example in [17]). However, the high resolution allows us to build a spatial picture of the temporal variability (inter-annual and seasonal), representing the coastal regions with high accuracy. This in turn highlights areas near the coast where the resource is the most consistent.

We focus on the 90, 100 and 125 m height levels, given that typical hub heights for offshore wind turbines are in this range [40]. In fact, the hub height of the wind farm installed in the Arklow Bank (in the Irish Sea [6]) is 124 m. In Figure 3, we present the annual and seasonal averages of wind power at the 100 m vertical level and the normalized standard deviation of the annual means which quantifies the inter-annual variability. The available wind power, P (W/m^2) per unit of swept area, is evaluated as:

$$P = \frac{\rho_{air} v^3}{2}, \tag{1}$$

where v is the wind speed and ρ_{air} is the density of air taken as 1.225 kg/m^3.

Looking at Figure 3, the wind energy density offshore is considerably greater than over land, even close to the coastline. This makes the future development of near-shore/coastal wind farms very attractive since offshore wind energy installations will offer a larger energy yield than land based wind farms.

The spatial variation of the wind energy resource is quite small offshore. Near the coast, the effect of the orography becomes more apparent. For example, in the greater Galway Bay area (from Mace Head down to the Dingle Peninsula, the area marked in Figure 3 boxes "W" and "SW"), and in Donegal Bay (in the box marked "NW"), there is orographic sheltering at a smaller scale than the resolution of ERA-Interm (79 km). This can also be seen along the east coast. It is clear that the downscaled HARMONIE model offers a considerably more accurate representation of nearshore wind energy

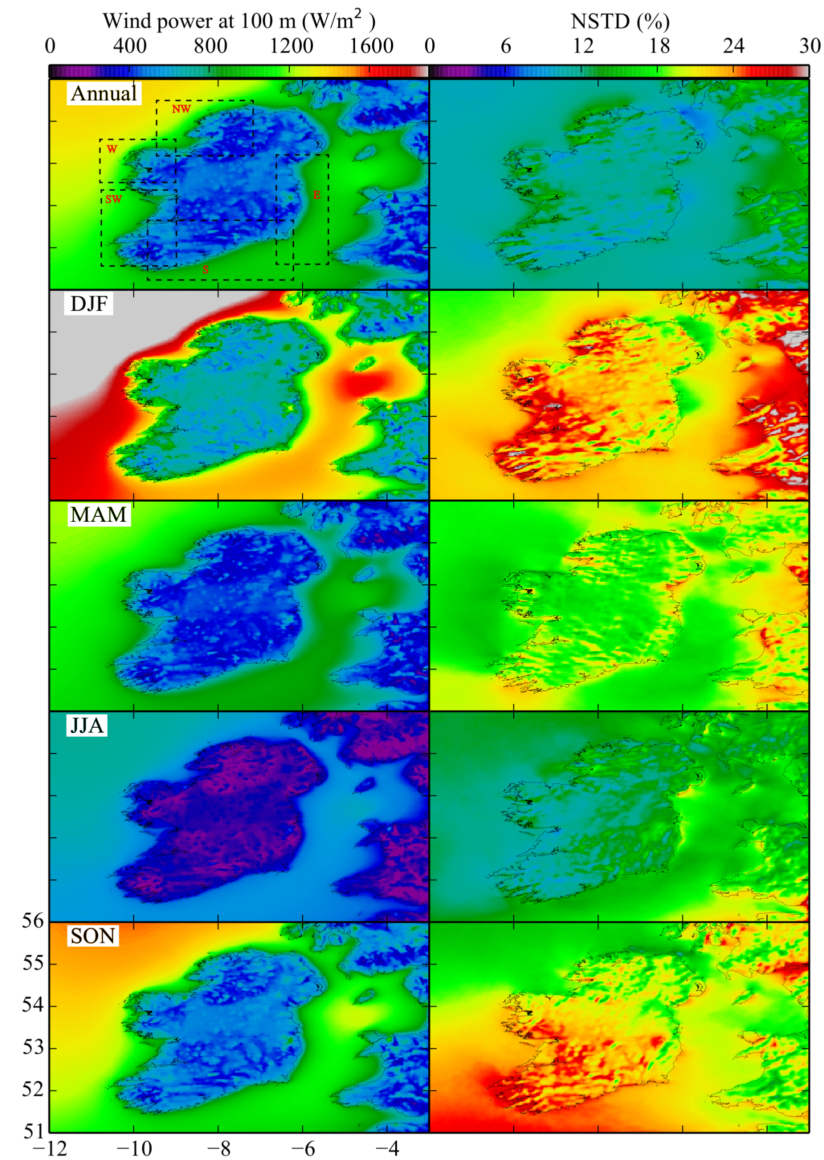

Figure 3: Wind power at 100 m for Ireland. Left panels show the averages (annual and seasonal means) and the right panels show the normalised standard deviation of the annual means (%) which is a measure of the interannual variability of the wind power resource.

levels.

Examining Figure 3, the strongest wind energy intensity is off the northwest of Ireland, coinciding with the northeast Atlantic storm track corridor [41]. Hurricane-force extra-tropical cyclones pass to the northwest of Ireland on average two to three times per year [42]. The east coast wind resource is more consistent, while still retaining relatively high wind power levels (generally a difference of 200-400 W/m^2, with respect to the west coast).

Proven offshore-wind technologies are foundation-based and can be deployed at depths of up to approximately 30 m for monopile structures, and 60 m for multi-pile structures. Floating bases would allow deployments at greater depths (up to 200 m); however these technologies are still under development [43, 7, 44, 45]. With this in mind, we looked at the spatial distribution of the wind energy in the nearshore focusing on its variability with respect to the bathymetric contours and distance to the shore. Furthermore, since the interplay between the predominant wind direction and coastal orography can induce a significant difference in the vertical profile of wind speeds (and therefore the energy resource) we looked at multiple hub-height vertical levels. Figures 4 to 6 display the seasonal averages of wind power at the 90 m level and the difference between the 125 m and 90 m levels, for the northwest and west; southwest and south; and east coast, respectively. The isobaths of 25, 50, 75 and 100 m are depicted in the figures.

The wind power is the strongest nationally in the northwest (Figure 4 (a)). Generally, there is little dissipation from the offshore (25-40 km away from the coastline, around the 75 m isobath) to the nearshore. In particular, the segment between Malin Beg and Tory Island offers high power density between the 25 m and 50 m isobaths, which are very close to the shoreline (less than 10 km). At the same time, note the close proximity to the North Atlantic storm track corridor, and the regular occurrence of the hurricane force winds associated with it [42]. The more sheltered Donegal Bay also offers good potential for wind farm installations, as it offers some degree of protection from the very harsh wind climate, in particular during winter. In general, the difference in energy between the 90 and 125 m levels varies with distance to the shore. Along the 75 m isobath, a difference of approximately 120 W/m^2 between the 90 and 125 m

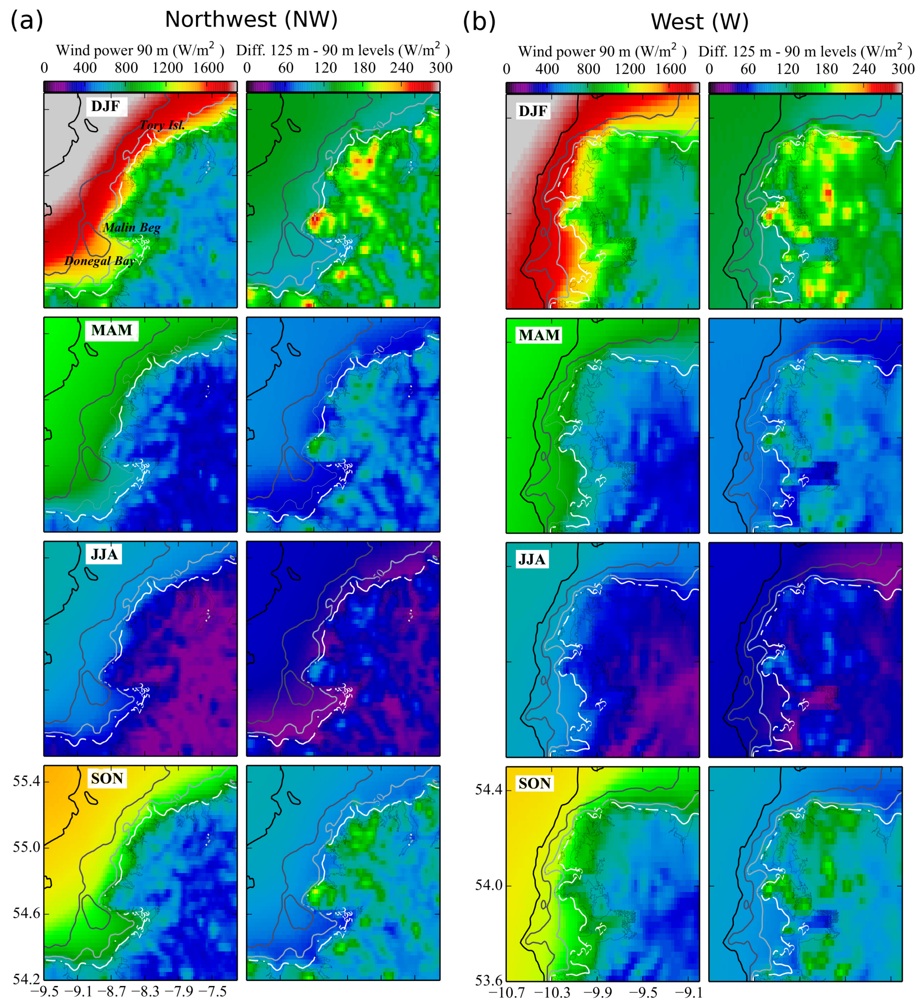

Figure 4: Seasonal averages of the wind power at 90 m (left panels) and the difference between the 125 m and 90 m levels (right panels) for (a) the northwest and (b) west coast of Ireland (area's marked NW and W in Figure 3).

levels can be seen in the winter, and 80-100 W/m^2 in autumn and spring. The seasonal variability is pronounced, with energy levels in the winter three times larger than those in the summer (still a substantial level of circa 600 W/m^2).

On the west coast (Figure 4 (b)) power levels almost as high as on the northwest coast can be seen, with the exception of the region to the east of Broadhaven Bay. We note considerable energy levels along the 75 m isobath, at its closest to the coastline, near the Mullet Peninsula (5 to 10 km). In fact, the power levels (at both 90 m and 125 m hub-heights) are consistent right up to the shoreline (depths of less than 25 m).

As we move southwards, from Galway Bay to the Dingle peninsula, (Figure 5 (a)) the power levels decrease, with the highest levels off Mace Head (the intended location of the Fuinneamh Sceirde Teoranta wind energy project) and off the tip of the Dingle Peninsula (the Blasket Islands). There is a marked decrease in energy levels from the offshore to the nearshore (around 30 %). When looking at the differences between the 90 m and 125 m vertical levels (right panels), in winter and autumn, the power levels at the 125 m are higher than at the 90 m level uniformly from the offshore to the nearshore (130 W/m^2 in winter, 80 W/m^2 in autumn). In spring and summer, the differences are reduced, and in fact, the reduction is not uniform and more pronounced in the nearshore. This fact could be linked to the marked seasonal variability in mean wind direction, at the level of the entire North Atlantic basin [46] and for Ireland, as can be seen in Figure 7 (a).

The south and east regions (Figures 5 (b) and 6, respectively) have similar wind energy levels, with quite uniform energy density distributions from the shoreline to the 50 m isobath. The only exception is off Carnsore point, where high wind energy densities can be seen, quite close to the shoreline. Note that in the Irish Sea, the area with depths under 50 m is large, and offers many potential locations for offshore wind farm sites (for example the four sites, either installed, or under development, marked in Figure 6). Note also, that on the east coast, the energy densities at the 90 and the 125 m vertical levels are similar along the 25 m isobath.

The mean seasonal 10m wind direction is shown in Figure 7 (a). The predominant direction on the west coast is southwesterly. However in the summer and spring, the direction is from the west (in spring, mainly in the Galway Bay region). On the east

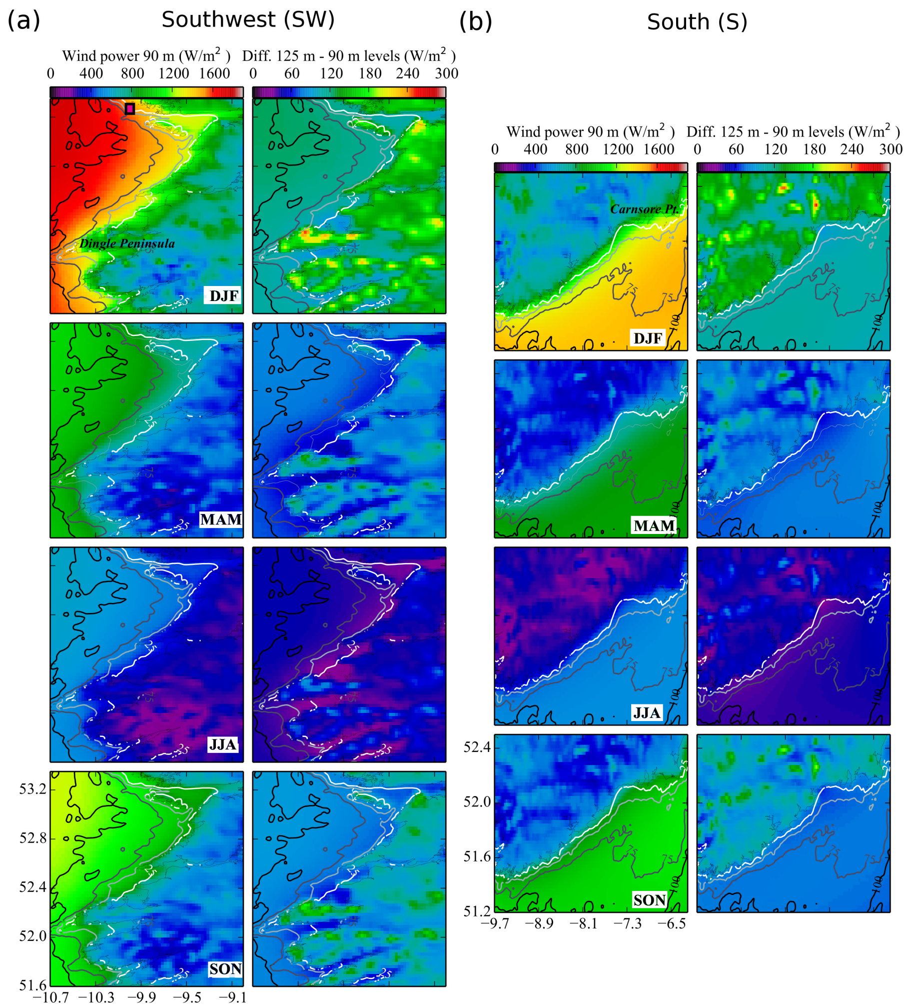

Figure 5: Seasonal averages of the wind power at 90 m (left panels) and the difference between the 125 m and 90 m levels (right panels) for (a) the southwest coast and (b) the south coast of Ireland (panel SW and S in Figure 3). The square marker shows the proposed position of the Fuinneamh Sceirde Teoranta wind energy project.

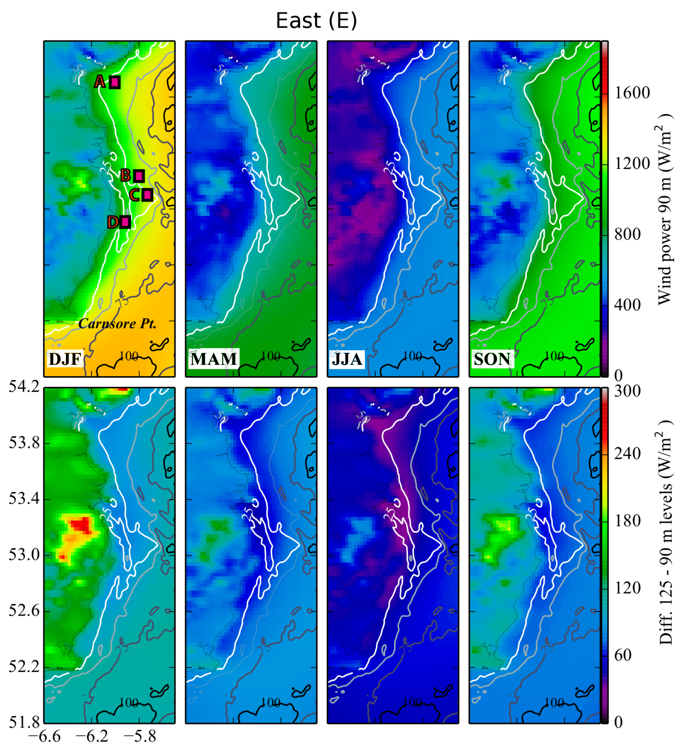

Figure 6: Seasonal averages of the wind power at 90 m (upper panels) and the difference between the 125 m and 90 m levels (lower panels) for the east coast of Ireland (area E marked in Figure 3). The square markers show the positions of the wind farm development projects in this region: A - Oriel Windfarm, B - Kish Bank, C - Codling and D - Arklow Bank array.

coast, wind direction is also from the southwest, with a southerly shift in spring and in summer (less pronounced). Such shifts in the wind direction will modify the sheltering patterns associated with the land topography of coastal regions and implicitly affect the seasonal characteristics of the nearshore wind energy resource. To show the directional spread around the coast, the directional distribution of the 10 m wind speed intensity at 6 locations on the 60 m isobath are depicted in Figure 7 (b). More directional spread is apparent in the west and southwest of Ireland.

So far we have looked at the inter-annual and seasonal variability in the wind energy resource. To gain an understanding of the distribution of wind speed regimes over a typical year and at typical hub heights, Weibull probability distribution functions (PDF) were fitted to model speeds at the 90 m and 125 m vertical levels, for the six points on the 60 m isobath (displayed in Figure 7 (b)) - see Figure 8. Points 1 and 2 on the west coast have the highest median speeds and the highest frequency of occurrence of extreme wind speeds, see in particular panels (b) and (d) of Figure 8, where the tails of the distributions are depicted. From these panels, the 125 m vertical level experiences more extreme wind speeds than the 90 m level as can be seen in the tail of the distribution. Note also that Point 6 in the Irish Sea has a higher probability of occurrence of speeds in the 20 to 30 m/s range than points 4 and 5 off the south and southwest coast.

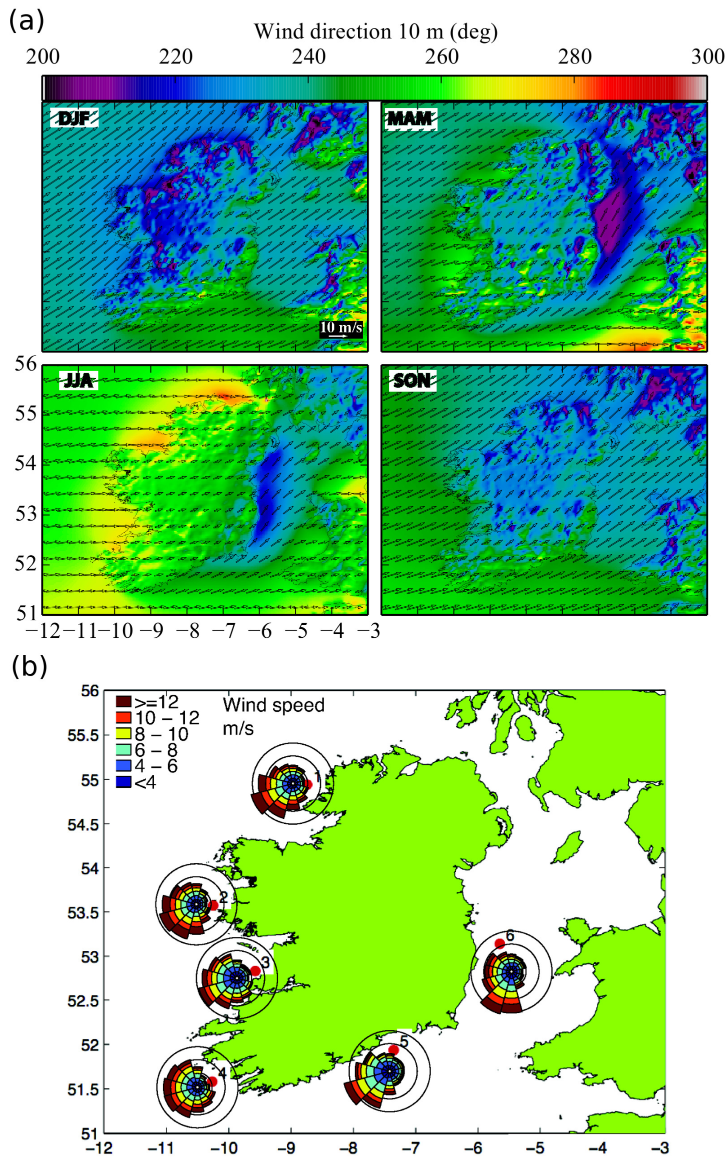

Figure 7: Directionality of the nearshore 10 m winds (a) Seasonal means of 10 m wind direction for Ireland (meteorological convention, 0° northerly, 90° easterly). Average velocity (average wind speed including direction) by season is overlaid using black directional arrows. The length of arrow for 10 m/s is depicted (in white) in the DJF panel for reference. (b) Frequency of occurrence of wind speeds grouped in directional bins (wind roses) at 6 locations around the Irish coast. The circles mark the levels of the 5 %, 10 % and 15 % frequency of occurrence.

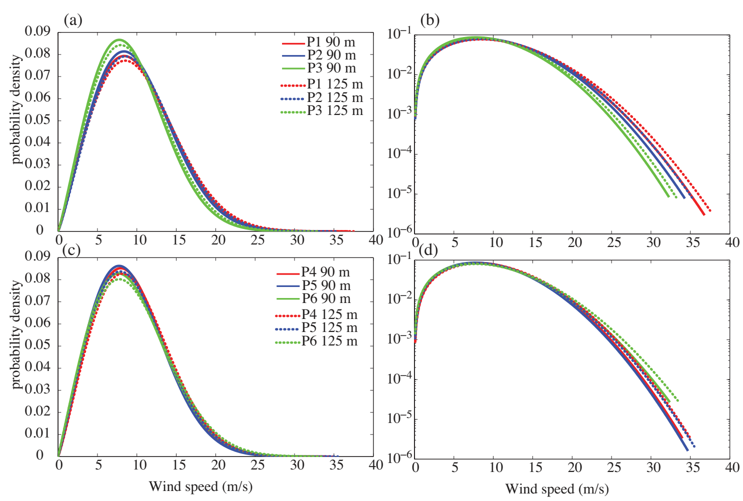

Figure 8: Weibull PDF fitted to wind speeds at the 90 m and 125 m levels at 6 locations around the Irish coast (points 1, 2, 3 upper panels and points 4, 5, 6 lower panels). The right panels display the PDF on a logarithmic scale to emphasize the tail of the distribution (high wind speeds, lower probability extreme events). The location of the points can be seen in Figure 7 (b), numbered and marked by red dots.

3.2. Wave resource

In this section, we present seasonal averages of wave power per metre of wave crest for Ireland (Figure 9) and maps focusing on areas of interest for wave energy installations in Figure 10. The wave power per metre of wave crest, J(W/m) is defined as follows:

$$J = \rho_w g E c_g \tag{2}$$

where ρ_w is the density of water, g is the acceleration due to gravity, E is the first moment of the frequency-direction spectrum and c_g is the average group velocity taken over the frequency–direction spectrum [23]. The response of most wave energy converters (WECs) varies at difference frequencies of excitation and their typical power capture performance will depend on the device characteristics, and the spectral shape and bandwidth of the spectral distribution of energy. For example, in the case of an Oscillating Wave Surge Converter (OWSC) such as the Oyster (size 20–25 m), the highest part of the power capture response is in the frequency range 0.085 Hz to 0.16 Hz [47]. Coupling the device performance characteristics with the typical wave conditions that could be expected at a site (on an annual average basis) the wave energy flux range of most interest is approximately 10–75 kW/m.

The west and south coasts are included in this analysis, although the power levels typically seen in these regions are low (compared to the west) and thus this area has not received much interest for potential WEC farm locations. At the same time, some studies [48] suggest that for lower power regimes (10–20 kW/m of wave front) the global technical wave energy levels (for all the regions with this level of resource) are estimated to be double those corresponding to the range 20–30 kW/m (100-500 TWh/year). It should be noted that the southern coast is exposed to wave power levels in the range 15–20 kW/m. The same levels are registered in many sheltered bay areas on the west coast.

Figure 9 (a) shows that the western seaboard experiences high-energy sea states (over 100 kW/m) particularly in winter, which diminish only slightly from the offshore in to the coast. Much of the energy in the winter on the west coast is comprised of large sea states, for which the amount of extractable energy may be constrained (due to the

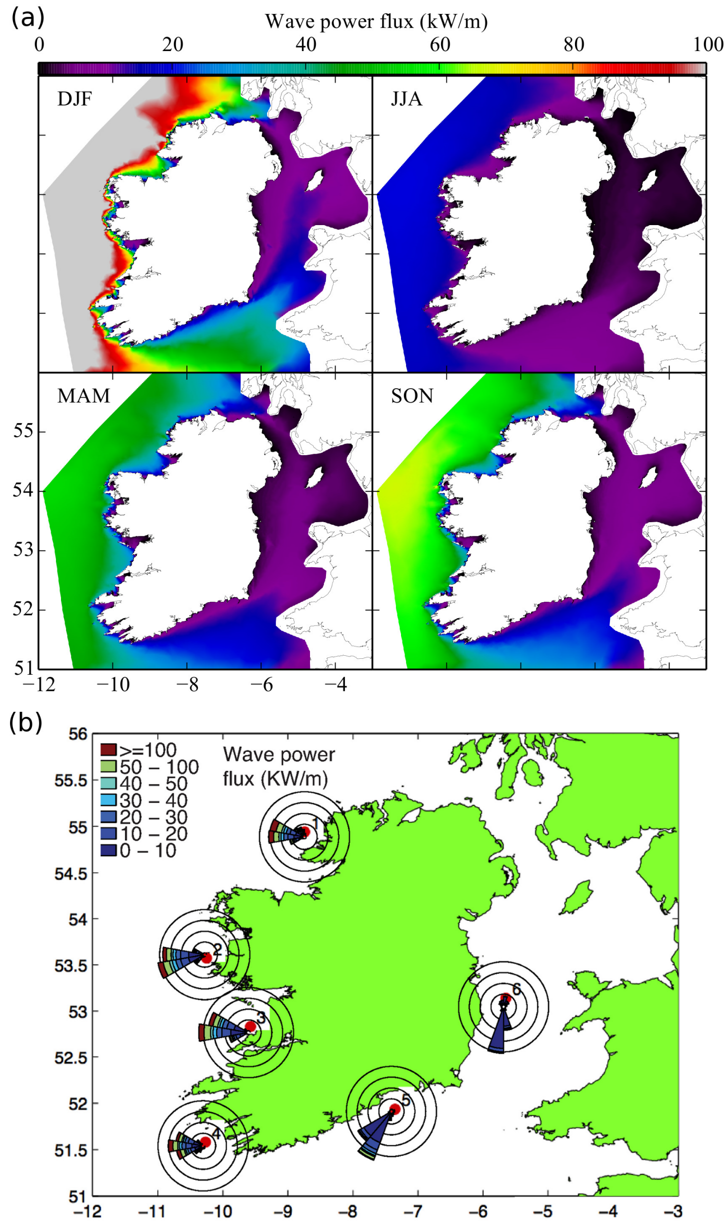

Figure 9: (a) Seasonal averages of wave power per metre of wave crest (kW/m) for Ireland. (b) Directionality of the wave energy resource. Histograms of the maximum directionally resolved wave power per metre of wave crest at 6 locations around the Irish coast. The circles mark the 10 %, 20 %, 30 % and 40 % frequency of occurrence levels.

design limits on WEC technologies). Thus, the exploitable energy [49] in the winter is substantially reduced. In the summertime substantial energy levels can still be seen on the west coast (up to 20 kW/m). The inter-annual variability of the wave resource is in the range of 20 to 35 % (largest in spring) as discussed in [8]. This is in contrast to the variability in the wind resource, which is smaller (in the range of 10 to 25 %). The largest variability in the wind power can be seen in the winter months – see Figure 3, right panels.

Assessment of the directionality of the wave energy resource is an important element for most WEC technologies, as it impacts both the deployment of the device and also the design process. The directionally-resolved wave power (defined as the energy flux through a surface with normal incidence to a particular direction) is a quantity often used to characterize directionality [50]. Histograms of the maximum directionally-resolved wave power and the corresponding directions are presented for 6 locations on the 60 m isobath around Ireland – see Figure 9 (b). On the west coast, a larger directional spread can be seen at the location 1 (north) and 4 (south) than at locations 2 and 3, with very similar frequency of occurrence of power levels between 20 and 100 kW/m. A slightly larger frequency of occurrence of power levels over 100 kW/m can also be seen at location 1. The frequency of occurrence of any power levels over 10 kW/m at location 6 on the east coast is much lower than at other locations. Power levels above 10kW/m occur more frequently at location 5 on the south coast.

The seasonal averages of wave energy flux for the northwest are depicted in Figure 10 (a). On the 25 m isobath, resource levels of 90 kW/m can be seen in winter from Malin Beg to Tory Island. The wind resource along this isobath is also very large as shown in Figure 4 (a). Two areas with exceptional power density, located very close to the shore (so called *hot spots* of wave energy) can be seen to the south of Arranmore Island and to the north of Malin Beg. These are areas where the wave energy resource is higher than would be otherwise expected for the water depth, due to wave interaction with irregular bathymetry or the steep sea-floor slope (see for example [51]). Donegal Bay has a smaller average wave energy levels available, with the wave power flux half of that of the more exposed coastline segment mentioned above, across all seasons. In winter, energy levels are 35-60 kW/m on average on the 50 m isobath in the bay (as

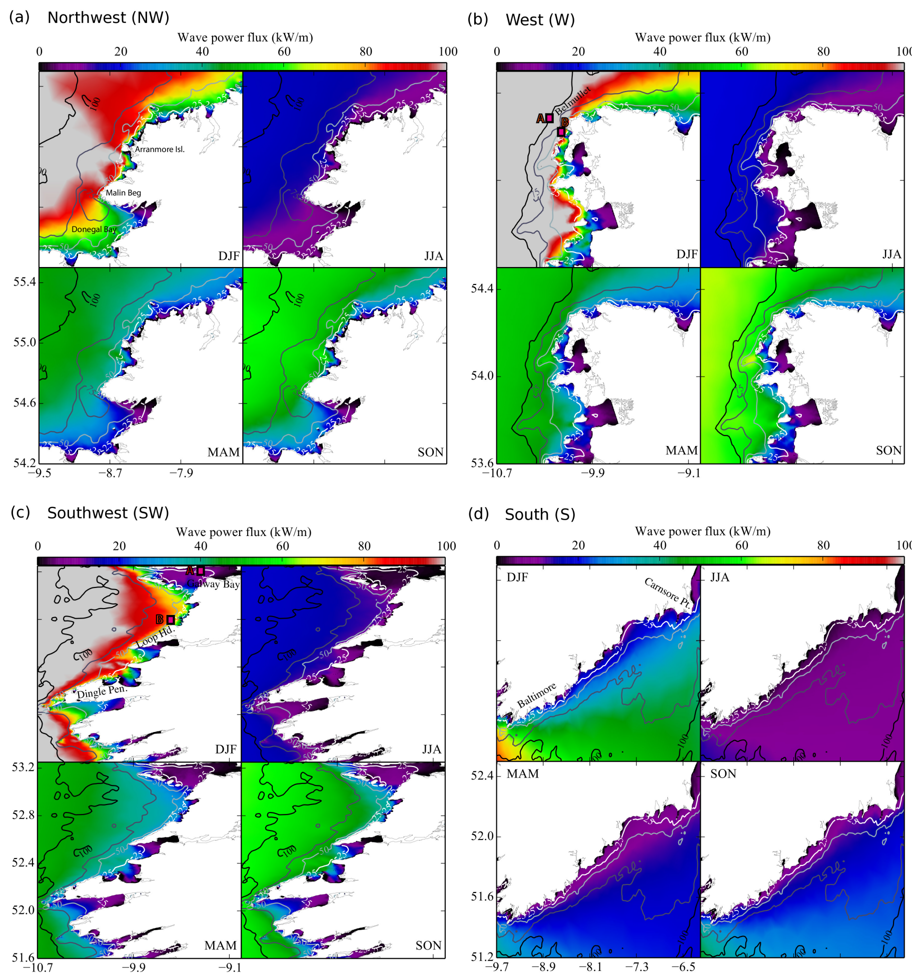

Figure 10: Seasonal averages of wave power per metre of wave crest (kW/m) for (a) the northwest, (b) the west, (c) the southwest and (d) the south coast of Ireland (panels NW, W, SW and S in Figure 3). In (b): the AMETS wave energy test sites are marked with squares: 'A' - the 100 m isobath and 'B' - 50 m isobath test area. In (c): 'A' the Galway Bay quarter scale test site and 'B' the WestWave Killard Point project location.

opposed to over 90 kW/m north of Malin Beg). In summer this ratio is again half, with 10 kW/m in the bay and 20 kW/m on the exposed coastline. The spatial distribution of wave energy density in autumn is similar to the one in spring for the northwest, with about 10 kW/m more energy offshore, in autumn, than in spring.

The west coast, south of Belmullet (see Figure 10 (b)), possesses the highest wave energy resource of any other region in Ireland. In fact, the area to the west of Belmullet depicted by markers A and B in Figure 10 (b), is the location of the AMETS full-scale wave energy test site. The amount of energy dissipation to the coastline is considerably less than in the northwest region. Wave energy flux levels remain high even in spring and autumn with 30–50 kW/m on the 25 m isobath.

The wave energy resource for the southwest region is shown in Figure 10 (c). Very high wave energy fluxes can be seen up to the 75 m isobath. The energy density decreases gradually to the shore, with the exception of the Dingle Peninsula and the segment between Killard Point and Loop Head. Galway Bay is sheltered somewhat from the energetic North Atlantic by the Aran Islands, with an energy levels of about 10 kW/m in the winter. This is the location of a 1/4-scale wave energy test site is marked by A in Figure 10 (c).

The season averages for the south coast are depicted in Figure 10 (d). In this region, the wave energy resource is substantially reduced compared to the other regions examined. Nonetheless, on the 50 m isobath, energy levels of about 20 kW/m are present in winter, and of at least 10 kW/m in the other seasons. The nearshore energy levels are largest off Carnsore Point and Baltimore, with the portion in between being more sheltered.

3.3. Correlation between the wind and wave energy resource

A challenge that both the wind and wave energy industries face is the inherent intermittence of the resource, which spans many time scales: from minutes to seasons to decades. In particular, high-frequency variability causes the biggest difficulty when integrating these resources into the power supply grid. One way to tackle this problem is to develop highly accurate met-ocean forecasts which in turn will enable fast-response grid-supply planning – see for instance [52, 53, 54] for wind forecasting.

In addition, wind and wave energy exploration can be combined to take advantage of the complementarity of the two resources in certain regions – as suggested for instance in [55, 56, 18, 19]. This has the potential to reduce transmission requirements. In order to assess the complementarity between the wind and wave energy resource around the Irish coast, and in particular in the nearshore, we have evaluated the correlation between the wave and wind power (following [55]) on the 30 and 60 m isobaths. As our main goal is to construct a spatial picture of the complementarity rather than an in-depth device-specific analysis (as in [55]) we have used the raw available power, not focusing on any particular technology. We extend the analysis in [55] (which had considered only three years of data from four offshore locations – M1, M2, M3 and the Kinsale Energy Gas platform, see Figure 2), to the entire extent of the Irish coast in the nearshore, and to a longer timeframe (2000–2013).

Thus, we have interpolated the wind and wave hindcast results for both the wave energy flux (with the finite-depth formula based on the variance spectra using Equation 2) and the wind power density at the 100 m vertical level from the HARMONIE meso-scale model (using Equation 1) to the two isobaths. Subsequently, we have evaluated the correlation between the resulting time series (with temporal resolution of 1 hour). The results are summarised in Figure 11.

Firstly, the offshore wind energy potential is quite consistent around the coast, with mean annual values between 800–1200 W/m^2. In contrast, the wave energy resource is much less consistent around Ireland with reasonable levels only available off the Atlantic coast and, to a lesser degree, off the Celtic Sea coast. The east coast offers excellent offshore wind potential, but no viable wave energy resource.

On the west coast, the wave and wind power are moderately correlated (correlation coefficients in the range 0.5–0.6). This is due to the fact that much of the wave energy resource here is not locally generated, consisting of swells originating from other regions of the North Atlantic basin. Our findings are consistent with [55]. Our analysis highlights segments around the western coast, close to the shore, where wind/wave combined farms could exploit the lag between energetic wind and wave resource availability and thus smooth out some of the high-frequency variably in the resource.

In sheltered areas such as Galway Bay and the northern part of the Donegal Bay,

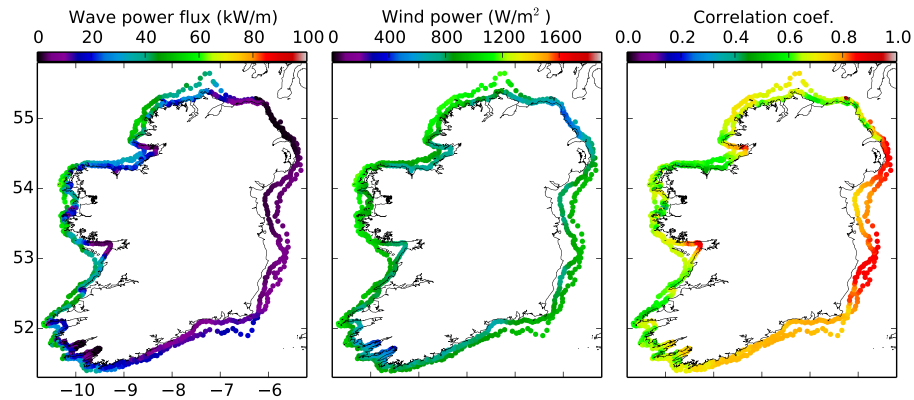

Figure 11: Left panel–mean wind power at the 100 m level (W/m^2), middle panel–mean wave power flux (kW/m) and right panel–correlation between wind power and wave energy flux. For this analysis, wave and wind hindcasts were interpolated to points on the 30 m and 60 m bathymetric contours.

the resource is due to local wind growth and thus is highly correlated to the wind power (correlation coefficients over 0.8[2]). On the south coast, the wind-wave correlation is higher than the west coast. The correlation coefficient of 0.7 indicates some complementarity. The wave energy levels on the 60 m isobath in this region, in particular off Carnsore Point and Baltimore, are substantially smaller than on the west coast, but still significant, making these sites good candidates for joint wind/wave farms.

4. Accessibility for marine operations

Site accessibility for marine operations (deployment and maintenance) is another great challenge for the marine renewable energy sector. Performing maintenance at sea is expensive and risky, as experience from the offshore oil industry and, more recently, the offshore wind industry suggests. Deployment and maintenance activities require sufficiently long time intervals with met-ocean parameters under certain thresholds (op-

[2] Incidentally, this is the case also on the east coast, where the wave-climate is wind-sea dominated. However, the wave energy resource here is too small for wind/wave farms to be a viable option.

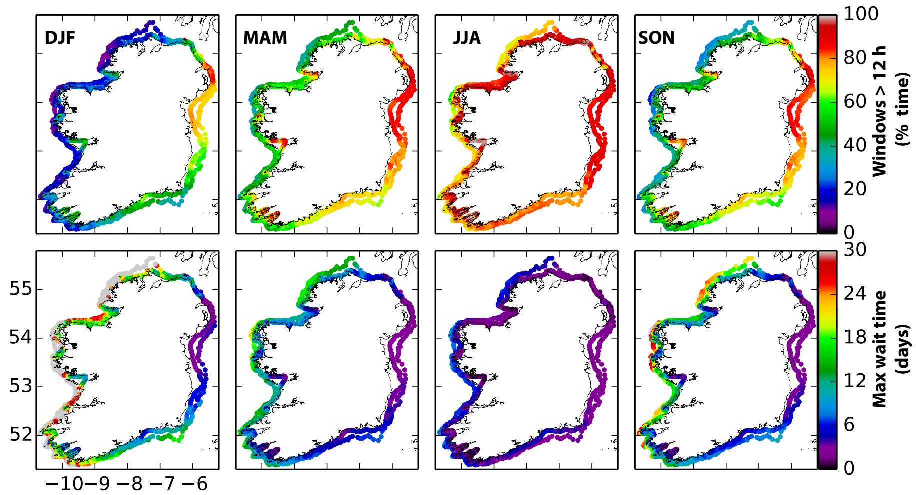

Figure 12: Upper panels: percentage of time comprising of weather windows larger than 12 hours for which wind speed is less than 16 m/s, Hs is less than 2 m and the peak period Tp less than 13 s respectively. Lower panels: average of the yearly maximum waiting time between weather windows satisfying the criteria above. For this analysis, wave and wind hindcasts were interpolated to points on the 30 m and 60 m bathymetric contours.

erational limits). These limits depend on the operation being performed and the type of vessel employed. In this section, we present a weather window analysis incorporating wind speeds, significant wave heights and peak periods. We focus on the nearshore, and more specifically locations along the 30 m and 60 m isobaths.

Our analysis closely follows the methodology described in [57], where a weather window analysis based on wind speeds, significant wave heights, wave periods and tidal currents was performed for three sites (the AMETS test site off the Belmullet peninsula in Ireland, the M2 buoy in the Irish Sea and the OWEZ wind farm site off the Dutch North Sea coast). However, that study was based on a limited dataset of measurements, spanning only a one year period.

We note that accessibility levels are sensitive to the thresholds, which depend on the specific vessel requirements [58]. However, as in Section 3.3, we aim to build a spatial picture of accessibility around the coastline, rather than an in-depth, device-specific analysis. Thus we considered a typical scenario corresponding to a generic jack-up vessel for offshore wind turbine installations (see for instance [57, 58], which provide operating limits in terms of significant wave height and wind speed). Furthermore, since recent studies [59] reveal that the wave period is also a limiting operating factor, we included a 13 second threshold for the peak period, in addition to a 2 m threshold for the significant wave height and 16 m/s for the wind speed. We neglected the tidal current in this analysis while recognising that it might play an important role in the Irish Sea.

The upper panels in Figure 12 display the percentage of time each season where there are weather windows satisfying the criteria mentioned above (Hs < 2 m, Tp < 13 s, wind speed < 16 m/s) and are of at least 12 hours length (a sufficiently long time to carry out marine operations). The lower panels show the maximum waiting times for access (taken as the average of the yearly maxima of waiting times between windows of at least 12 hours length, a measure of the 'worst case scenario' waiting time in each season).

In winter, on the west coast, accessibility windows amount to less than 20 % overall. Less than 10 % accessibility can be seen off the Belmullet Peninsula (where the AMETS wave energy testing site is located) and around Malin Beg. The maximum waiting times exceed a month on the 60 m isobath in many parts of this region, and are generally greater than 18 days on the 30 m isobath. Nonetheless, the north part of Donegal Bay and Galway Bay have access levels of around 40 % in winter with maximum waiting times of around 18 days on the 30 m isobath. At the same time, the wind energy resource here has high levels and the wave energy resource in not negligible (in particular in Donegal Bay) - see Figure 11.

In contrast, on the east coast, even in winter, accessibility levels exceed 50 % (even 60 % where the Arklow Bank offshore wind farm is located). Maximum waiting times on the east coast are less than a week even in winter time (three days or less in the other seasons).

South coast accessibility levels in winter are lower than on the east coast but are still significant: 50–60 %, with maximum waiting times of approximately 12 days. The exposed extremal points (off Baltimore and Carnsore Point) are exceptions, with maximum waiting times of over 18 days in winter.

In summer [3], accessibility levels are generally over 70 % all around the coast. The only exception is Belmullet, were access levels remain under 60 % along the 60 m isobath.

The accessibility levels in spring are similar to autumn, on the south and east coasts. On the west coast, autumn has reduced accessibility levels with respect to the spring season (circa 40 % versus 50 %), with maximum waiting times of 24 days, in the northwest, and off the Belmullet peninsula.

[3]Interestingly, in summer on the south coast, the access levels on the 30 m isobath are slightly less than on the 60 m isobath (still, maximum waiting times less than 6 days). This can be attributed to the 13 s threshold chosen for the peak wave period. Indeed, the 90^{th} percentile of the peak period in summer is slightly above this threshold on the 30 m isobath, and about 12 s (below the threshold) for the 60 m isobath. Hence, the Tp threshold is more likely to be exceeded on the 30 m isobath. This anomaly demonstrates the sensitivity of accessibility levels to the Tp threshold, and implies that Tp limit should be linked to the wave height.

5. Discussion

In this section, we discuss the wind and wave energy resource around the coast while taking into account accessibility levels. The wind energy resource is consistent around the coast as can be seen in Figure 11, middle panel - with annual averages reaching 1200 W/m^2 on the 60 m isobath off the northwest coast, and values of circa 800 W/m^2 on the east coast. On the 30 m isobath off the south coast, there is a small drop in the energy density (100-200 W/m, most likely due to sheltering effects) compared to the east coast. On the 60 m isobath however, the energy levels are comparable to those on the east coast. When accessibility is taken into account, the east coast stands out as a preferred location for offshore wind farm developments. In fact, the majority of planned developments are concentrated on the east coast (see Figure 6). At the same time, grid integration and infrastructure are readily available there, where much of the population is located.

The south coast also offers reasonable accessibility levels, with only slightly less wind energy levels available than off the east coast. The west coast has some low accessibility, particularly in winter, with the exception of more sheltered areas such as Galway Bay and Donegal Bay. It should be noted that the location of the Fuinneamh Sceirde Teoranta wind energy project (see Figure 5) has slightly higher accessibility levels compared to the more exposed areas. The directionality of the wind (Figure 7) was also examined, and was shown to play an important role in the wind power resource in coastal areas that experience orographic sheltering effects.

In contrast to the wind energy resource, the wave resource is restricted to the Atlantic coast and off the Celtic Sea coast (with smaller levels, but still significant). Notably, the Belmullet area (where the AMETS tests site is located, see Figure 10 (b)) and the northwest benefit from exceptional levels of wave energy. However, these regions are quite exposed and problems with accessibility may occur (as Figure 12 reveals). Other sites that stand out as potential locations for WEC farms, with only slightly smaller wave energy levels but slightly higher accessibility, are south of Achill Island and the area from Killard Point (potential site for the WestWave project [3]) down to the Dingle peninsula.

Our study highlights sites around the coast that might have been overlooked in terms of potential for wind, wave or combined wind/wave energy installations. The energy resource at these locations has reasonable levels, and more importantly they are somewhat sheltered from the extreme North Atlantic climate (see Figure 1 for locations):

1. West of Malin Head, where excellent wave (30–40 kW/m annual average) and wind (over 800 W/m^2 annual average) energy resources can be seen along the 30 m isobath. The accessibility along the 60 m isobath is low in this region (as Figure 12 shows). Thus, suitable locations for WEC or offshore wind development are in shallower water depths (30 m or less), where accessibility is reasonable: the maximum waiting time in winter is approximately 12 days. The correlation between the wind and wave energy resource is also relatively low (0.6) indicating some complementarity between the two.
2. Donegal Bay has significant levels of wave energy resource (20 kW/m annual average on the 30 m isobath and up to 40 kW/m annual average on the 60 m isobath) and wind (600–800 W/m^2 annual average), with good complementarity between the two (approximately 0.6 correlation). Here the accessibility levels are among the best on the west coast.
3. The Dingle Peninsula has exceptional levels of both wave and wind energy in the nearshore. However low accessibility can be seen in parts of the peninsula. The complementarity between the wave and wind energy is the best on the west coast (correlations range between 0.5→0.6).
4. Regions off the south coast such as Carnsore Point and Baltimore (near to Sherkin Island) have similar wind energy levels to the east coast, and small but significant levels of wave energy resource (20 kW/m annual average). The accessibility levels are better than on the west coast. Complementarity between the wind and wave energy resource is reduced (correlation of circa 0.7).

We have considered accessibility strictly from a meteorological perspective, without considering the proximity to the existing grid infrastructure and port facilities. We stress that many of these sites are in isolated locations without appropriate grid infrastructure, or nearby ports of access. This will have a great impact on site selection [60, 2]. Long-term planing on the part of policy makers is required to provide the infrastructure necessary for the energy resource in such locations to be exploited for the benefit of Ireland.

6. Summary and Conclusions

A 14-year high resolution wave and wind hindcast was carried out for Ireland, and validated against available buoy, synoptic station and altimeter data. The wind was dynamically downscaled from the ERA-Interim reanalysis (approximately 80 km horizontal resolution and 60 vertical levels) to a 2.5 km horizontal grid spacing and 65 vertical levels, using the HARMONIE meso-scale model [22, 25]. The wave hindcast was derived using WAVEWATCH III [23] on an unstructured grid with a resolution ranging between 10 km offshore and 225 m in the nearshore. The wind forcing consisted of the downscaled HARMONIE 10 m wind speeds and the boundary wave spectra from the ECMWF ERA-Interim reanalysis.

The temporal extent of 14 years of the wind and wave hindcasts enabled us to perform an analysis of the seasonal and inter-annual variability and derive reliable estimates of power distribution. However, the 14-year duration is not sufficient to characterize variability of the climate on scales of decades or more, and these variations need to be taken into account for future planning. It should be noted that, at least for the wave energy resource, the inter-annual variability is significantly larger than decadal variations [61, 62]. A study of the long-term wave climate of Ireland and its inter-decadal variability was carried out in [8].

Apart from estimating the wind and wave energy resource, in the current study we have considered the nearshore wind and wave climate in conjunction with each other, and highlighted two issues that have relevance for the ocean renewable energy industry. Firstly, we have investigated the complementarity between the wind and wave energy resource in the nearshore (on the 30 m and 60 m isobaths around the entire coast). Areas with low correlation could be targeted as locations for joint wind/wave power farms to mitigate against the high-frequency variability in both resources.

Secondly, we assessed the accessibility for marine operations around the coast. In terms of accessibility, we identified three weather-window regimes around Ireland – see Figure 12: (i) the Atlantic coast, low accessibility levels, with a maximum waiting time of almost a month between access windows in winter, in most parts, (ii) the south coast, moderate accessibility levels, (iii) the east coast, high accessibility levels.

By ensuring that wind and wave conditions were considered jointly for this wind and wave climatology, we have been able to build a unified description of the wave and wind nearshore energy potential of Ireland and to select regions that have both a high energy density and are reasonably accessible for marine operations and maintenance. Based on this joint approach, we have recommended four new locations in the nearshore which might be suitable locations for joint wind/wave farms based on: (*i*) accessibility; (*ii*) the correlation between wind and wave; (*iii*) and the energy resource available.

In conclusion, this study addresses the uncertainty regarding the wind and wave renewable energy potential in Irish coastal areas. It provides detailed information on wind and waves that reflects the current climate (2000–2013), an important consideration in view of climate change over past decades. This adds to the Irish national capacity to inform commercial interests involved in marine operations in general, and in exploiting ocean renewable energy.

Finally, we plan to produce a new atmospheric dataset for Ireland (MÉRA – Met Éireann Reanalysis) by improving and building on the work carried out for this study. This reanalysis will run from the period 1979 to the present using HARMONIE, with both surface and upper air data assimilation and a larger model domain.

Appendix A. Hindcast Validation

Appendix A.1. Validation of HARMONIE winds

In this section we present a validation study of the HARMONIE 10 m winds used to force the wave model by comparison with observations from three classes of station (locations shown in Figures 1 and 2): (*i*) measurements from the M-buoys from the the Irish Marine Weather Buoy Network (details in Table A.1) in order to examine the

Station	*Latitude* $^\circ N$	*Longitude* $^\circ W$	*Period* (mm/yy)
M1	53.127	11.200	01/01-12/07
M2	53.480	5.425	05/01-12/12
M3	51.217	10.551	02/07-12/12
M4	54.998	9.992	05/07-12/12
M4 old location	54.667	9.066	12/03-05/07
M5	51.689	6.701	10/04-12/12
Bellmulet	54.228	10.004	01/00-12/12
Mace Head	53.317	9.900	04/10-12/12
Malin Head	51.940	10.237	01/00-12/12
Sherkin Island	55.372	7.338	04/10-12/12
Valentia	51.476	9.428	01/00-12/12

Table A.1: The location of the stations and the duration of time series of observations used in the comparison with HARMONIE and ERA-Interim model 10 m wind output. The M-stations denote the Irish marine buoys and the last 5 stations are the subset of synoptic coastal land stations examined in detail in Figure A.13. The locations of the stations can be seen in Figure 1 (a).

performance of the model offshore; (*ii*) measurements across all synoptic land and buoy stations available over the hindcast period for the UK and Ireland (over 120 stations) and (*iii*) measurements from a subset of 5 synoptic weather stations located in coastal areas around Ireland (in order to focus on the performance of the model in regions of potential interest for renewable energy applications in the nearshore).

Additionally, we present a comparison of the station observations with the ERA-Interim Re-analysis 10 m winds, in order to quantify the improvement in the high-resolution HARMONIE winds with respect to the forcing data set. The quality indexes for the comparison of model to observations are shown in Figure A.13. We have displayed the paired-in-time quality index plots comparing (*a*) HARMONIE (hourly-forecasts from the 00, 06, 12 and 18 hour model runs) to observational data, by forecast length and (*b*) ERA-Interim and the HARMONIE forecasts (using the 0, 3 and 6-hour forecasts from the 00 hour and 12 hour model runs) to observations. We have also used all available observations from the synoptic coastal land stations for the hindcast period 2000-2012.

The bias, root mean square error (RMSE) were compared for both wind speed and direction – a summary of selected results are shown in Figure A.13. The bias is defined as the mean of the difference between observed data, x_i, and model data, y_i over n number of observation/data pairs:

$$Bias = \frac{1}{n}\sum_{i=1}^{n}(x_i - y_i) \tag{A.1}$$

In this case a negative bias means that the model is greater than the observations. Note that the relative bias (%) is the bias divided by the mean of the observed data, $\frac{Bias}{\bar{x}} \times 100$. The root mean squared error (RMSE) is calculated by evaluating the deviations of the model points from the observations, summing these and taking the square root:

$$RMSE = \sqrt{\left(\frac{1}{n}\sum_{i=1}^{n}(x_i - y_i)^2\right)} \tag{A.2}$$

Finally, the HARMONIE output was also validated by comparing the relative bias and scatter index against satellite wind speed measurements from the CERSAT altimeter database [38], obtained from the Centre de Recherche et d'Exploitation Satellitaire (CERSAT), at Ifremer. The scatter index (SI) is defined as the root mean square error divided by the mean of the observations, $\bar{x}$. This can be shown as a percentage (%) by multiplying by 100.

$$SI = \frac{RMSE}{\bar{x}} \tag{A.3}$$

Appendix A.1.1. Marine buoys

The quality indexes for the comparison of model to observations are shown in Figure A.13 (a). This analysis extends a validation study performed in [10] where 10 m ERA-Interim and ECMWF operational archive winds were compared to M1, M3, M5 and M6 buoy measurements. All available measurements from 2000 to 2012 from M buoys were used in the validation study shown in Figure A.13 (a); (geographical locations depicted in Figure 1 (a)). The station coordinates and periods of available measurements for the M buoys are summarised in Table A.1. The temporal resolution of all observations is 1 hour. The buoy measurements are not continuous, with data missing for several months during the period. Furthermore, the wind speeds are truncated to the closest 1 knot for the marine buoys and synoptic stations. Such truncations can increase the scatter between the model and observations [63]. HARMONIE and ERA-Interim wind fields were bilinearly interpolated to the station locations.

The buoy wind measurements were adjusted from the anemometer height (4.5 m for the Marine Institute buoys [64]) to 10 m using a logarithmically varying profile correction for wind speed with height assuming neutrally stable atmospheric conditions [65]:

$$v(z) = v_r(z_r)\frac{ln\left(z/z_0\right)}{ln\left(z_r/z_0\right)}, \tag{A.4}$$

where v is the wind speed at height z, v_r is the known wind speed at height z_r and z_0 is the sea surface roughness length, taken to be 2×10^{-4} m.

The downscaled HARMONIE winds generally exhibit smaller biases and RMSEs in both wind speed and direction relative to ERA-Interim. As can be seen in Figure A.13 (b), RMSE values are less than 2 m/s and biases mostly less than -0.5 m/s. Significant reductions in directional bias were also found for the buoys located closer to the shoreline (not shown): at the M2 buoy from $-9°$ to $-3°$, at the M4 old location from $-8°$ to $-5°$ and at the M5 buoy from $-6°$ to $-3°$ respectively. These gains in resolving directionality are evident in Figure A.14 where directional histograms of wind speed intensities are displayed. Furthermore, ERA-Interim underpredicts wind-speeds at these locations, in particular for strong intensity regimes. This bias is considerably reduced by the HARMONIE downscaling, as the wind roses in Figure A.14 show.

Appendix A.1.2. Land stations

All available measurements from 2000 to 2012 from the subset of 5 coastal land stations (shown in Figure A.13 (a)) were used in the validation study. Additionally, the HARMONIE model was validated over the same period against all available data from the more than 120 stations (denoted in Figure A.13 (b)). The improvements brought

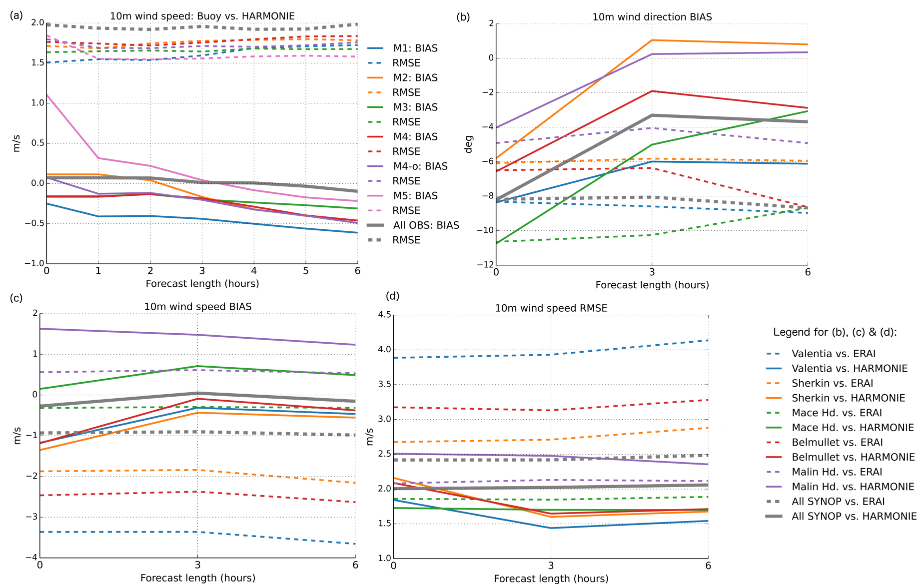

Figure A.13: (a) Verification of the HARMONIE versus M buoys for 10 m wind speeds (from the 00, 06, 12 and 18 hour model runs) to observational data (compared hourly). (b) 10 m wind directional biases of the HARMONIE and ERA-Interim versus the subset of 5 coastal land station observational data (and the total of all the available station observations in the model domain – see Figure 1 (a) and (b), respectively). Solid lines show the HARMONIE versus measured results; dashed lines show the ERA-Interim scores versus the observations from the 0, 3 and 6-hour forecasts from the 00 hour and 12 hour model runs. (c) Same as (b) but for 10m wind speed bias and (d) RMSE.

by the HARMONIE downscaling are, as expected, more prominent at the coastal land stations, with overall smaller RMSEs in both wind speed and direction. Biases are also reduced for the speed and direction, with the exception of Malin Head where only the directional bias is reduced (to close to zero – see Figure A.13 (b)). Although the RMSE is improved for Mace Head, the bias is marginally worse when compared to ERA-Interim (Figure A.13 (c)), however, the directional bias has reduced to $-3°$ from $-9°$ by the 6-hour forecast. These are less sheltered (more exposed) stations and therefore the model improvement in these biases (due to the better resolved local orography) may not have as pronounced an effect.

Overall, a reduction in the bias of 1 m/s and the RMSE of 0.5 m/s for the 10 m wind speed; and 4° in the directional bias was found for all surface stations combined versus HARMONIE, compared to ERA-Interim. The histograms of wind speed intensities (Figure A.15) show the better performance of the HARMONIE model in capturing directionality and lower wind speeds regimes at Mace Head.

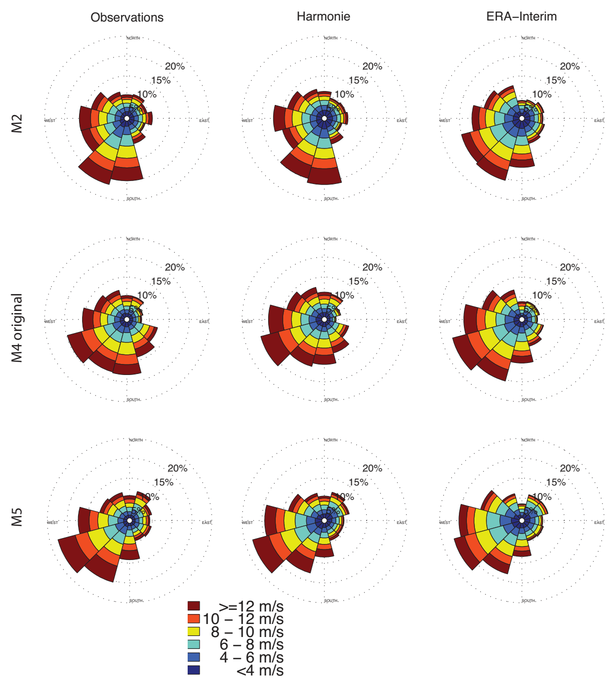

Figure A.14: Wind roses for the 10 m wind speed (m/s) at the M2, M4 (original) and M5 marine buoys: observations for the time-periods described in Table A.1 (left), HARMONIE (center) and ERA-Interim (right).

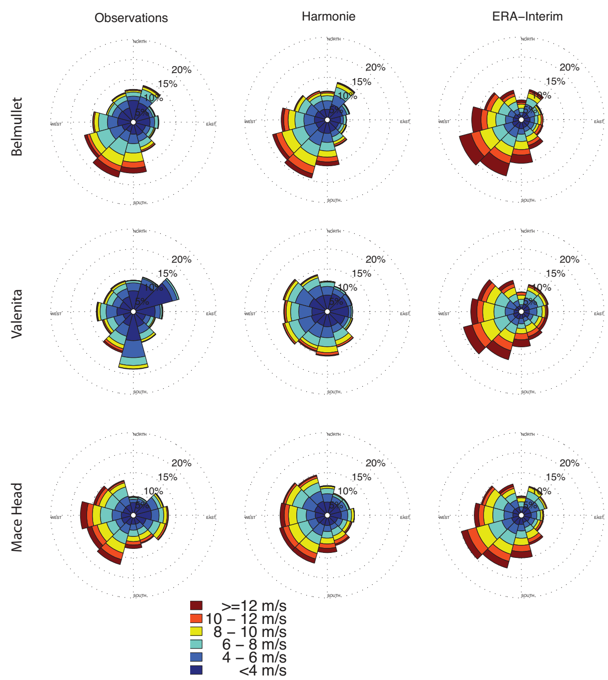

Figure A.15: Wind roses for the 10 m wind speed (m/s) from January 2010–October 2011 at three of the coastal land stations: observations (left), HARMONIE (center) and ERA-Interim nearest sea-point (right).

Altimeter data

The CERSAT altimeter database was produced in the framework of the Globwave project [66], funded by the European Space Agency (ESA). Altimeter data in the CERSAT database are available from as far back as 1991 when the European Space Agency (ESA) launched the ERS-1 (followed in 1992 by the CNES/NOAA TOPEX/ Poseidon missions [39]) up until the present day. A list of the satellite campaigns used for the comparison can be seen in Table 3 of [8]. All available altimeter data over the hindcast period were included.

In summary, the overall statistical indexes using all available altimeter measurements over the model domain are: bias 0.03 m/s (the overall mean being 8.86 m/s) and RMSE 1.66 m/s. The HARMONIE downscaling has reduced the bias compared to the forcing dataset (see [8], where we have compared ERA-Interim 10 m winds to altimeter measurements over the same model area, but for the period 1992–2012). The quality of the HARMONIE dataset is further confirmed in Figure A.16, where scatter and quantile-quantile (Q-Q) plots are displayed along with spatial quality index maps. As can be seen in Figure A.16 (a), the altimeter derived and HARMONIE 10 m winds agree well for wind speeds less than 20 m/s. The algorithms to estimate the wind speed have been developed for data up to 20m/s, and therefore cannot measure winds above 20 m/s reliably [67]. The relative bias shown in Figure A.16 (c), is mostly within ±10% with a slightly larger bias near to the coastline in the Celtic and Irish Seas. The SI, shown as a percentage in Figure A.16(d), is generally under 20% off the west coast and under 25% in the Irish Sea.

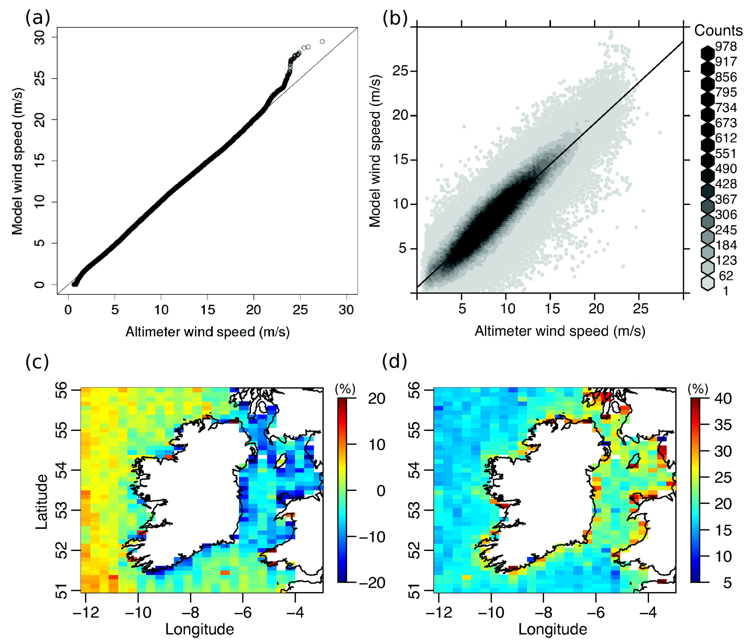

Figure A.16: (a) Q-Q plot, (b) scatter plot, (c) relative bias quality index map and (d) scatter (shown as %) quality index map for the 10 m wind speed altimeter vs. HARMONIE (for the period 2000-2013). The relative bias (%) is defined in Equation A.1 and the SI (%) in Equation A.3.

Appendix A.2. Validation of WAVEWATCH III

The wave model was validated with data from 18 wave buoys located around the Irish coastline as shown in Figure 2. We grouped the available data in to two categories: (*i*) off-shore buoys (water depths ranging from 70 m to 155 m) and (*ii*) near-shore buoys (water depths ranging from 11 m to 60 m) – see Table A.2. The WAVEWATCH III output was also validated against satellite significant wave height (Hs) measurements from the CERSAT altimeter database [38].

Appendix A.2.1. Marine buoys

The statistical indexes for model versus observations for Hs, period and direction are displayed in Table A.3. All directional error statistics were calculated using the circular statistics MATLAB toolbox from [68]. The quality indexes generally reveal good agreement of the model with measurements. The correlation coefficients for Hs exceed 0.9.

The performance of the model was found to be comparable to the 34 year hindcast by [69, 8] which was forced with ERA Interim 10 m winds. Nonetheless, we note improvements in areas where the wind-sea regime is dominant: at the G1 buoy in Galway bay (a reduction in bias for Hs of 7 cm to 0 cm), and in the Irish Sea (M2: a reduction in Hs bias from 15cm to 1.8 cm, directional bias from −15 cm to −8 cm and an increase in correlation from 0.84 to 0.88). Off the south coast (the M5 buoy) a reduction in the directional bias from −6 cm to −4 cm and an increase in correlation from 0.77 to 0.79 can also be seen. These could be attributed to the use of high-resolution HARMONIE downscaled winds. Note that the model exhibits a reasonable agreement with the measurements from the G1 buoy (located in the Galway Bay, at a depth of 22 m). This buoy is the only nearshore consistent data set available, spanning a period of approximately 3 years. The longest observational wave record available (almost 14 years, covering the full span of the wave hindcast) is from the Kinsale Energy Gas platform (KIN) in the Celtic Sea. The model displays good agreement with this time-series – see Table A.3.

Buoy	*Location*	*Latitude* $^\circ N$	*Longitude* $^\circ W$	*Depth* (*m*)	*Period* (*mm/yy*)
M3	SW of Mizen Head	51.217	10.551	155	01/03 - 12/12
M4	Donegal Bay, offshore	54.998	9.992	155	05/07 - 12/13
M1	W of Aran Isl.	53.127	11.200	140	03/01 - 12/07
BH4	W of Belmullet	54.285	10.270	100	05/12 - 12/12
M2	E of Lambay Isl.	53.480	5.425	95	05/03 - 12/13
Kinsale energy gas platform	Celtic Sea	51.366	8.000	90	01/00 - 12/13
M4, old location	Donegal Bay, nearshore	54.667	9.067	72	04/03 - 05/07
M5	SE Coast	51.689	6.701	70	10/04 - 12/12
BH3	W of Belmullet	54.231	10.146	56	12/09 - 01/12
K1	Killard Point	52.762	9.621	51	11/11 - 01/12
AC1	Achill Isl.	53.864	10.052	43	11/11 - 08/12
BH1	Broadhaven Bay	54.303	9.901	38	01/09 - 10/09
K2	Killard Point	52.766	9.579	36	08/12 - 12/12
SB2	E of Aran Isl.	53.114	9.511	28	01/10 - 06/10
G1	Galway Bay	53.227	9.271	22	05/08 - 01/12
AC2	Achill Isl.	53.899	10.010	21	11/11 - 01/12
SB1	Mace Head	53.333	9.932	18	04/09 - 09/09
BH2	Broadhaven Bay	54.290	9.841	11	06/06 - 07/09

Table A.2: The locations of the buoys, the depth and the duration of time series of observations used in the comparison with model data shown in Table A.3. Buoys are listed in order of depth. SW = south-west, W = west, E = east. The location of the buoys around the Irish coastline are shown in Figure 2.

Appendix A.2.2. Altimeter data

A supplementary method to verify the wave model's performance is to compare to satellite-derived wave data. This offers a robust validation tool in the open ocean, up to tens of km from the coast, as data in the coastal zone are considered unreliable and are often discarded. Altimeter measurements are in fact invaluable in regions where little or no buoy data are available, such as in the Irish Sea (M2). Similarly to the analysis in Appendix A.1.2, we have assessed the wave model's quality by comparison to the CERSAT altimeter database [38]. The database was calibrated and corrected for bias by [39].

The spatial quality index maps can be seen in Figure A.17 along with the Q-Q and scatter plots for Hs. The overall statistical indexes show good agreement with altimeter data at the level of the entire model domain: bias 2 cm (the mean altimeter Hs being 2.33 m), RMSE 38 cm and correlation coefficient 0.97. These indexes show a slight

Buoy	Significant wave height $\overline{X}$ (m)	$Bias$ (cm)	$RMSE$ (cm)	SI	r	Period $\overline{X}$ (s)	$Bias$ (s)	$RMSE$ (s)	SI	r	Direction $\overline{X}$ (deg)	$Bias$ (deg)	$RMSE$ (deg)	SI	r
M3	2.86	−5.4	45	0.16	0.96	6.93	−0.07	0.74	0.11	0.88	275	5	19	0.15	0.95
M4	3.06	−3.5	41	0.13	0.97	6.92	−0.08	0.66	0.09	0.90	277	5	13	0.16	0.92
M1	2.94	−16.5	46	0.16	0.96	6.95	−0.11	0.67	0.10	0.89					
BH4	2.87	5.2	39	0.13	0.96	6.65	−0.16	0.53	0.08	0.93	291*	9	20	0.30	0.70
M2	1.20	1.8	30	0.25	0.94	4.47	0.56	0.90	0.20	0.72	193	−8	21	0.13	0.79
KIN	2.02	3.1	29	0.14	0.97	5.39	−0.16	0.65	0.12	0.88					
M4 (old)	2.34	−30.5	59	0.25	0.94	6.72	−0.03	0.80	0.12	0.87					
M5	1.81	−11.4	41	0.22	0.94	5.48	−0.15	0.74	0.13	0.85	231	−4	16	0.12	0.88
BH3	2.77	10.6	40	0.15	0.97	7.03	−0.17	0.69	0.10	0.90	296*	8	16	0.26	0.69
K3	3.55	11.3	49	0.14	0.97	7.76	−0.34	0.80	0.10	0.88	287*	10	13	0.18	0.84
K1	4.57	21.4	48	0.10	0.97	8.02	−0.36	0.63	0.08	0.89	291*	5	9	0.13	0.73
AC1	2.32	−16.5	36	0.15	0.98	6.30	−0.64	0.96	0.15	0.92	270*	5	13	0.14	0.69
BH1	1.90	2.6	31	0.16	0.97	6.19	−0.32	0.86	0.14	0.89	317	2	9	0.21	0.88
K2	2.44	19.6	39	0.16	0.96	6.67	−0.39	0.82	0.12	0.91	292*	0	9	0.13	0.76
SB2	0.62	−11.7	20	0.32	0.90	4.33	−0.53	1.52	0.35	0.71	269	10	27	0.27	0.64
G1	0.75	0.0	16	0.21	0.96	4.09	−0.33	1.25	0.30	0.70	230*	10	19	0.15	0.52
AC2	3.79	6.6	44	0.12	0.95	12.30*	−0.38	1.45	0.12	0.76	256	6	11	0.10	0.36
SB1	0.85	−48.2	57	0.68	0.96	4.68	−0.96	1.36	0.40	0.75	231	4	12	0.10	0.69
BH2	0.36	−16.8	26	0.72	0.97										

Table A.3: Comparison between the model and buoy data for significant wave height, period and direction: the mean of the buoy ($\overline{X}$), the bias, the root-mean square error ($RMSE$), the scatter index (SI) and the correlation coefficient (r) are shown. Where possible, the zero-crossing period and mean direction were used. The quality indexes are defined in Equations A.1 – A.3. At some locations, no directional measurements, or only the peak period or peak direction were available. All directional error statistics were calculated using the circular statistics toolbox from [68]. *(* denotes where comparisons were between the buoy and model peak period or peak direction, respectively.)*

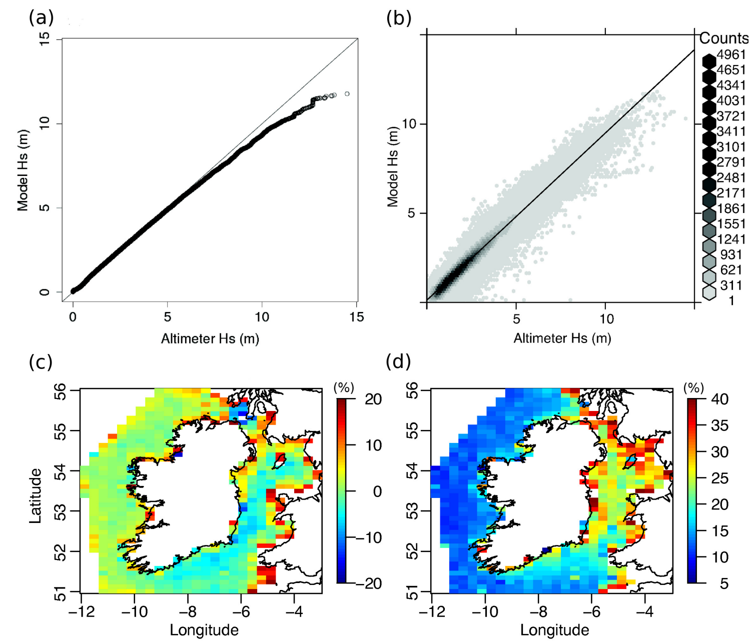

Figure A.17: (a) Q-Q plot, (b) scatter plot, (c) relative bias quality index map and (d) scatter (shown as %) quality index map for significant wave height altimeter vs. wave hindcast (for the period 2000-2 013). For the relative bias (%), see Equation A.1, and for the SI (%), see Equation A.3.

improvement with respect to the hindcast in [8][4]: a reduction in bias from 7 cm to 2 cm and in RMSE from 39 cm to 38 cm. When looking at the spatial bias areal map in Figure A.17 (c), it is evident that this improvement is largely concentrated in the Irish Sea where relative biases were reduced from approximately 10 % (under-estimation of Hs by the model) to around ±5 % in this study.

Acknowledgements

This study was funded by Science Foundation Ireland (SFI) under the research project "High-end computational modelling for wave energy systems" (10/IN.1/I2996)

[4]The hindcast in [8] was driven by ERA-Interim and validated with the entire extent of the altimeter database (from 1992 to 2012).

and by the Sustainable Energy Authority of Ireland (SEAI) through the Renewable Energy Research Development & Demonstration Programme (RE/OE/13/20132074). The ESB, Met Éireann, the Marine Institute and Shell provided the buoy data for validation. The INFOMAR bathymetric datasets were provided by the Geological Survey Ireland (GSI) and the Marine Institute. The VORF software for tidal datum conversions was obtained from the GSI. The UKHO bathymetry was provided by Ocean-Wise Ltd. The authors thank the ECMWF for providing the ERA-Interim Re-analysis data. The altimeter-derived wave data was obtained from the Centre de Recherche et d'Exploitation Satellitaire (CERSAT), at Ifremer, Plouzané, France in the frame of the Globwave project, funded by the European Space Agency (ESA). The authors thank Dr. C. Sweeney and Prof. P. Lynch (UCD School of Mathematical Sciences) for helpful discussions, Dr. F. Ardhuin (Ifremer) for his advice regarding the WAVEWATCH code and Dr. K. Dohery (Aquamarine Power) for providing useful information about the Oyster WEC. Finally, the numerical simulations were performed on the Stokes and Fionn clusters at the Irish Centre for High-end Computing (ICHEC) and at the Swiss National Computing Centre under the PRACE-2IP project (FP7 RI-283493) "Nearshore wave climate analysis of the west coast of Ireland". We would also like to thank the anonymous reviewers for their useful comments and suggestions.

Bibliography

[1] Dept. of Communications, Energy and Natural Resources, Delivering a Sustainable Energy Future for Ireland, Irish Government White Paper. `http://www.environ.ie/en/Publications/Environment/Atmosphere/FileDownLoad,1519,en.pdf`, [Online] (March 2007).

[2] Dept. of Communications, Energy and Natural Resources, The Offshore Renewable Energy Development Plan, OREDP. `http://www.dcenr.gov.ie/NR/rdonlyres/836DD5D9-7152-4D76-9DA0-81090633F0E0/0/20140204DCENROffshoreRenewableEnergyDevelopmentPlan.pdf`, [Online] (February 2014).

[3] WestWave, ESB WestWave project (2013) [cited 27 September 2013].
URL http://www.westwave.ie/

[4] MaREI, Marine Renewable Energy Ireland SFI Research Centre (MaREI) (2014) [cited 27 September 2013].
URL http://www.marei.ie

[5] The European Wind Energy Association (EWEA), 4.9 GW of new offshore wind capacity under construction in Europe [retrieved online 20/07/2014] (2014).
URL http://www.ewea.org/news/detail/2014/07/14/49-gw-of-new-offshore-wind-capacity-under-construction-in-europe/

[6] Dept. of Communications, Energy and Natural Resources, Offshore renewable energy offshore renewable energy offshore renewable energy. Stakeholder forum., Irish Offshore wind. http://www.dcenr.gov.ie/Energy/Sustainable+and+Renewable+Energy+Division/Offshore.htm [online], [Online] (July 2014).

[7] The National Offshore Wind Association of Ireland, Offshore Wind Ireland [retrieved online 26/07/2014] (2014).
URL http://www.nowireland.ie/offshore-wind-ireland.html

[8] S. Gallagher, R. Tiron, F. Dias, A long-term nearshore wave hindcast for Ireland: Atlantic and Irish Sea coasts (1979–2012), Ocean Dynamics 64 (8) (2014) 1163–1180. doi:10.1007/s10236-014-0728-3.
URL http://dx.doi.org/10.1007/s10236-014-0728-3

[9] S. Gallagher, R. Tiron, F. Dias, A detailed investigation of the nearshore wave climate and the nearshore wave energy resource on the west coast of Ireland, in: Proceedings of the ASME 2013 32nd International Conference on Ocean, Offshore and Arctic Engineering OMAE13, Nantes, France, 2013.

[10] R. Tiron, S. Gallagher, F. Dias, The influence of coastal morphology on the wave climate and wave energy resource of the West Irish Coast, in: Proceedings of

the 10th European Wave and Tidal Energy Conference Series EWTEC, Aalborg, Denmark, 2013.

[11] A. Rute Bento, P. Marinho, R. Campos, C. Guedes Soares, Modelling wave energy resources in the Irish West Coast, in: Proceedings of the 30th International Conference on Ocean, Offshore and Artic Engineering OMAE12, Rotherdam, Netherlands, 2012.

[12] ESB, Accessible wave energy resource atlas of Ireland., Tech. Rep. Report 4D404A-R2 for the Marine Institute and Sustainable Energy Ireland, ESB International (2005).

[13] M. Curé, A fifteen year model based wave climatology of Belmullet, Ireland, Tech. rep., A report prepared on behalf of the Sustainable Energy Authority of Ireland (SEAI). (2011).

[14] B. Cahill, A. Lewis, Long term wave energy resource characterization of the Atlantic Marine Energy Test Site., in: Proceedings of the 9th European Wave and Tidal Energy Conference, Southampton, U.K., 2011.

[15] SEI, Wind atlas 2003. report no. 4y103a-1-r1. `http://www.sei.ie/uploadedfiles/RenewableEnergy/IrelandWindAtlas2003.pdf` [retrieved online], Tech. rep., Sustainable Energy Ireland (SEI) (2003).

[16] S. M. Uppala, P. W. KÅllberg, A. J. Simmons, U. Andrae, V. D. C. Bechtold, M. Fiorino, J. K. Gibson, J. Haseler, A. Hernandez, G. A. Kelly, X. Li, K. Onogi, S. Saarinen, N. Sokka, R. P. Allan, E. Andersson, K. Arpe, M. A. Balmaseda, A. C. M. Beljaars, L. V. D. Berg, J. Bidlot, N. Bormann, S. Caires, F. Chevallier, A. Dethof, M. Dragosavac, M. Fisher, M. Fuentes, S. Hagemann, E. Hólm, B. J. Hoskins, L. Isaksen, P. A. E. M. Janssen, R. Jenne, A. P. Mcnally, J.-F. Mahfouf, J.-J. Morcrette, N. A. Rayner, R. W. Saunders, P. Simon, A. Sterl, K. E. Trenberth, A. Untch, D. Vasiljevic, P. Viterbo, J. Woollen, The ERA-40 re-analysis, Q. J. R. Meteorol. Soc. 131 (612) (2005) 2961–3012. doi:10.1256/qj.04.176.
URL `http://dx.doi.org/10.1256/qj.04.176`

[17] P. Nolan, P. Lynch, R. McGrath, T. Semmler, S. Wang, Simulating climate change and its effects on the wind energy resource of Ireland, Wind Energy 15 (4) (2012) 593–608. doi:10.1002/we.489.
URL http://dx.doi.org/10.1002/we.489

[18] E. D. Stoutenburg, N. Jenkins, M. Z. Jacobson, Power output variations of co-located offshore wind turbines and wave energy converters in California, Renewable Energy 35 (12) (2010) 2781 – 2791. doi:http://dx.doi.org/10.1016/j.renene.2010.04.033.
URL http://www.sciencedirect.com/science/article/pii/S0960148110002004

[19] E. D. Stoutenburg, M. Z. Jacobson, Reducing Offshore Transmission Requirements by Combining Offshore Wind and Wave Farms, IEEE J. Oceanic Engineering 36 (4) (2011) 552 – 561. doi:http://dx.doi.org/10.1109/JOE.2011.2167198.

[20] D. P. Dee, S. M. Uppala, A. J. Simmons, P. Berrisford, P. Poli, S. Kobayashi, U. Andrae, M. A. Balmaseda, G. Balsamo, P. Bauer, P. Bechtold, A. C. M. Beljaars, L. van de Berg, J. Bidlot, N. Bormann, C. Delsol, R. Dragani, M. Fuentes, A. J. Geer, L. Haimberger, S. B. Healy, H. Hersbach, E. V. Hólm, L. Isaksen, P. Kållberg, M. Köhler, M. Matricardi, A. P. McNally, B. M. Monge-Sanz, J.-J. Morcrette, B.-K. Park, C. Peubey, P. de Rosnay, C. Tavolato, Thépaut, J.-N., F. Vitart, The ERA-Interim reanalysis: configuration and performance of the data assimilation system, Q. J. R. Meteorol. Soc. 137 (656) (2011) 533–597. doi:10.1002/qj.828.

[21] HIRLAM, HIRLAM, http://www.hirlam.org (2013).

[22] Y. Seity, P. Brousseau, S. Malardel, G. Hello, P. Bénard, F. Bouttier, C. Lac, V. Masson, The AROME-France Convective-Scale Operational Model, Mon. Wea. Rev. 139 (3) (2011) 976–991. doi:10.1175/2010MWR3425.1.

[23] H. Tolman, User manual and system documentation of Wavewatch III version 4.18, Tech. Rep. 316, NOOA/NWS/NCEP/MMAB (2014).

[24] A. Roland, Development of WWM II: Spectral wave modelling on unstructured meshes, Ph.D. thesis, Institute of Hydraulics and Wave Resource Engineering, Technical University Darmstadt, Germany (2008).

[25] P. Brousseau, L. Berre, F. Bouttier, G. Desroziers, Background-error covariances for a convective-scale data-assimilation system: AROME–France 3D-Var, Q. J. R. Meteorol. Soc 137 (2011) 409–422. doi:10.1002/qj.750.

[26] A. Persson, User guide to ECMWF forecast products, Tech. rep., European Centre for Medium-Range Weather Forecasts (ECMWF), Shinfield Park, Reading, RG2 9AX, UK (October 2011).

[27] T. T. Warner, R. A. Peterson, R. E. Treadon, A tutorial on lateral boundary conditions as a basic and potentially serious limitation to regional numerical weather prediction, Bull. Amer. Meteor. Soc. 78 (1997) 25992617. doi:10.1175/1520-0477(1997)078,2599:ATOLBC.2.0.CO;2.

[28] L. M. Harris, D. R. Durran, An Idealized Comparison of One-Way and Two-Way Grid Nesting, Mon. Wea. Rev. 138 (2010) 2174–2187. doi:10.1175/2010MWR3080.1.

[29] T. Davies, Lateral boundary conditions for limited area models, Q.J.R. Meteorol. Soc. 140 (2013) 185196. doi:10.1002/qj.2127.

[30] H. Hollweg, U. Bhm, I. Fast, B. Hennemuth, K. Keuler, E. Keup-Thiel, M. Lautenschlager, S. Legutke, K. Radtke, B. Rockel, M. Schubert, A. Will, M. Woldt, C. Wunram, Ensemble Simulations over Europe with the Regional Climate Model CLM forced with IPCC AR4 Global Scenarios, Tech. Rep. 3, Max-Planck Institute for Meteorology, Model and Data (2008).

[31] G. Burgers, P. Baas, H. van den Brink, Towards an extreme wind climatology for The Netherlands based on downscaling ERA-Interim with the HARMONIE-AROME high-resolution model, poster presented at EGU 2013, Vienna (2013).

[32] TU - Darmstadt, Polymesh 2-D Mesh Generator: Manual and Quick Start Guide, Tech. rep., TU - Darmstadt (2012).

[33] F. Ardhuin, E. Rogers, A. Babanin, J.-F. Filipot, R. Magne, A. Roland, A. van der Westhuysen, P. Queffeulou, J.-M. Lefevre, L. Aouf, F. Collard, Semi-empirical dissipation source functions for wind-wave models: part I, definition, calibration and validation, J. of Phys. Oceanogr. 40 (9) (2010) 1917–1941.

[34] EMODnet, EMODnet, http://www.emodnet-hydrography.eu/content/content.asp?menu (2013).

[35] INFOMAR, Integrated Mapping for The Sustainable Development of Ireland's Marine Resource (INFOMAR): A Successor to the Irish National Seabed Survey. Proposal & strategy, Dublin, Ireland, 2006.

[36] OSI, Ordnance Survey Ireland, http://www.osi.ie/ (2013).

[37] LANDSAT, Global mosaic of Landsat7. courtesy nasa/jpl-caltech (2013) [cited 27 September 2013].
URL http://ows.geogrid.org/basemap

[38] CERSAT, Centre de Recherche et d'Exploitation Satellitaire (CERSAT), http://cersat.ifremer.fr/ (2013) [cited 21 December 2013].
URL http://cersat.ifremer.fr/

[39] P. Queffeulou, D. Croizé-Fillon, Global altimeter SWH data set, Tech. Rep. 10, Ifremer, Brest, ftp://ftp.ifremer.fr/ifremer/cersat/products/swath/altimeters/waves/documentation/altimeter_wave_merge__10.0.pdf (May 2013).

[40] F. Pimenta, W. Kempton, R. Garvine, Combining meteorological stations and satellite data to evaluate the offshore wind power resource of Southeastern Brazil, Renewable Energy 33 (11) (2008) 2375–2387.

[41] I. Franco-Trigo, Climatology and interannual variability of storm-tracks in the Euro-Atlantic sector: a comparison between ERA-40 and NCEP/NCAR reanalyses, Climate Dynamics 26 (2-3) (2006) 127–143. doi:10.1007/s00382-005-0065-9.
URL http://dx.doi.org/10.1007/s00382-005-0065-9

[42] J. A. Hanafin, Y. Quilfen, F. Ardhuin, J. Sienkiewicz, P. Queffeulou, M. Obrebski, B. Chapron, N. Reul, F. Collard, D. Corman, E. B. de Azevedo, D. Vandemark, E. Stutzmann, Phenomenal Sea States and Swell from a North Atlantic Storm in February 2011: A Comprehensive Analysis, Bulletin of the American Meteorological Society 93 (12) (2012/05/25) 1825–1832.
URL http://dx.doi.org/10.1175/BAMS-D-11-00128.1

[43] M. Bilgili, A. Yasar, E. Simsek, Offshore wind power development in Europe and its comparison with onshore counterpart, Renewable and Sustainable Energy Reviews 15 (2) (2011) 905 – 915. doi:http://dx.doi.org/10.1016/j.rser.2010.11.006.
URL http://www.sciencedirect.com/science/article/pii/S1364032110003758

[44] S.-P. Breton, G. Moe, Status, plans and technologies for offshore wind turbines in europe and north america, Renewable Energy 34 (3) (2009) 646 – 654. doi:http://dx.doi.org/10.1016/j.renene.2008.05.040.
URL http://www.sciencedirect.com/science/article/pii/S0960148108002243

[45] M. J. Dvorak, C. L. Archer, M. Z. Jacobson, California offshore wind energy potential, Renewable Energy 35 (6) (2010) 1244 – 1254. doi:http://dx.doi.org/10.1016/j.renene.2009.11.022.
URL http://www.sciencedirect.com/science/article/pii/S0960148109004984

[46] I. Young, Seasonal variability of the global ocean wind and wave climate, International Journal of Climatology 19 (9) (1999) 931–950. doi:10.1002/(SICI)1097-0088(199907)19:9¡931::AID-JOC412¿3.0.CO;2-O.
URL http://dx.doi.org/10.1002/(SICI)1097-0088(199907)19:9<931::AID-JOC412>3.0.CO;2-O

[47] D. Clabby, A. Henry, M. Folley, T. Whittaker, The effect of the spectral distribution of wave energy on the performance of a bottom hinged flap type wave energy

converter, in: Proceedings of the ASME 2012 31st International Conference on Ocean, Offshore and Arctic Engineering OMAE12, Rio de Janeiro, Brazil, 2012.

[48] H. Bernhoff, E. Sjosstedt, M. Leijon, Wave energy resources in sheltered sea areas: a case study of the Baltic Sea, in: Fifth European Wave Energy Conference, Cork, Ireland, 2003.

[49] M. Folley, T. Whitthaker, Analysis of the nearshore wave energy resource, Renew. Energy 34 (2009) 1709–1715.

[50] M. Folley, A. Cornett, B. Holmes, P. Lenee-Bluhm, P. Liria, Standardizing resource assessment for wave energy convertes., in: Proceedings of the 4th International Congress on Ocean Energy, Dublin, Ireland, 2012.

[51] G. Iglesias, R. Carballo, Wave energy and nearshore hot spots: The case of the SE Bay of Biscay, Renew. Energy 35 (11) (2010) 2490–2500. doi:http://dx.doi.org/10.1016/j.renene.2010.03.016.

[52] C. P. Sweeney, P. Lynch, P. Nolan, Reducing errors of wind speed forecasts by an optimal combination of post-processing methods, Meteorological Applications 20 (1) (2013) 32–40. doi:10.1002/met.294.
URL `http://dx.doi.org/10.1002/met.294`

[53] C. Sweeney, P. Lynch, Adaptive post-processing of short-term wind forecasts for energy applications, Wind Energy 14 (3) (2011) 317–325. doi:10.1002/we.420.
URL `http://dx.doi.org/10.1002/we.420`

[54] J. Courtney, P. Lynch, C. Sweeney, High resolution forecasting for wind energy applications using bayesian model averaging, Tellus A 65 (0).
URL `http://www.tellusa.net/index.php/tellusa/article/view/19669`

[55] F. Fusco, G. Nolan, J. V. Ringwood, Variability reduction through optimal combination of wind/wave resources: An Irish case study, Energy 35 (1) (2010) 314 – 325. doi:http://dx.doi.org/10.1016/j.energy.2009.09.023.

URL http://www.sciencedirect.com/science/article/pii/S0360544209004095

[56] A. Babarit, H. B. Ahmed, A. Clement, V. Debusschere, G. Duclos, B. Multon, G. Robin, Simulation of electricity supply of an atlantic island by offshore wind turbines and wave energy converters associated with a medium scale local energy storage, Renewable Energy 31 (2) (2006) 153 – 160, marine Energy. doi:http://dx.doi.org/10.1016/j.renene.2005.08.014.
URL http://www.sciencedirect.com/science/article/pii/S0960148105002223

[57] M. O'Connor, D. Burke, T. Curtin, T. Lewis, G. Dalton, Weather windows analysis incoporating wave height, wave period, wind speed and tidal current with relevance to deployment and maintenace of marine renewables., in: Proceedings of the 4th International Congress on Ocean Energy, Dublin, Ireland, 2012.

[58] M. O'Connor, T. Lewis, G. Dalton, Weather window analysis of Irish west coast wave data with relevance to operations and maintenance of marine renewables., Renewable Energy 52 (2013) 57–66.

[59] P. Augener, H. Hatecke, Sea keeping analysis of an offshore wind farm installation vessel during the jack-up process., in: Proceedings of the ASME 2014 33nd International Conference on Ocean, Offshore and Arctic Engineering OMAE14, San Francisco, USA, 2014.

[60] Irish Maritime Development Office, Marine Institute, A Review of Irish Ports Offshore Capability in Relation to Requirements for the Marine Renewable Energy Industry, IMDO Ireland. http://oar.marine.ie/bitstream/10793/838/1/IMDOIPORESReport.pdf, [Online] (August 2011).

[61] S. P. Neill, M. R. Hashemi, Wave power variability over the northwest european shelf seas, Applied Energy 106 (0) (2013) 31 – 46. doi:http://dx.doi.org/10.1016/j.apenergy.2013.01.026.
URL http://www.sciencedirect.com/science/article/pii/S0306261913000354

[62] E. B. Mackay, A. S. Bahaj, P. G. Challenor, Uncertainty in wave energy resource assessment. part 2: Variability and predictability, Renewable Energy 35 (8) (2010) 1809 – 1819. doi:http://dx.doi.org/10.1016/j.renene.2009.10.027.
URL http://www.sciencedirect.com/science/article/pii/S0960148109004534

[63] H. Bidlot, J-R, Verification of operational global and regional wave forecasting systems against measurements from moored buoys, JCOMM 30, World Meteorological Organization (2006).

[64] NOAA, NOAA National Data Buoy Center, http://www.ndbc.noaa.gov/station_page.php?station=62095&unit=M (2013).

[65] R. B. Stull, An introduction to boundary layer meteorology, Kluwer Academic Press, 1988.

[66] GlobWave, GlobWave project, http://www.globwave.org/ (2013) [cited 21 December 2013].
URL http://www.globwave.org/

[67] S. Zeiger, J. Vinoth, I. Young, Joint Calibration of Multiplatform Altimeter Measements of Wind Speed and Wave Height over the Past 20 Years, J. Atmos. Oceanic Technol. 26 (2009) 2549–2564. doi:http://dx.doi.org/10.1175/2009JTECHA1303.1.

[68] P. Berens, CircStat: a MATLAB toolbox for circular statistics., J. of Statistical Softw. 31 (10).

[69] S. Gallagher, R. Tiron, F. Dias, A 34-year Nearshore Wave Hindcast for Ireland (Atlantic and Irish Sea Coasts): Wave Climate and Energy Resource Assessment, in: Proceedings of the 13th International Workshop on Wave Hindcasting and Forecasting and 4th Coastal Hazards Symposium, Environment Canada, the Canadian Federal Program of Energy R&D, and the WMO/IOC Joint Technical Commission for Oceanography and Marine Meteorology (JCOMM), http:

//www.waveworkshop.org, Banff, Canada, 2013. URL http://www.waveworkshop.org/13thWaves/index.htm/